Characteristics of Ultrasonic Ranging Sensors in an Underground Environment

By W. H. Strickland and R. H. King

UNITED STATES DEPARTMENT OF THE INTERIOR

BUREAU OF MINES

Report of Investigations 9452

Characteristics of Ultrasonic Ranging Sensors in an Underground Environment

By W. H. Strickland and R. H. King

UNITED STATES DEPARTMENT OF THE INTERIOR
Bruce Babbitt, Secretary

BUREAU OF MINES

Library of Congress Cataloging in Publication Data:

CONTENTS

ILLUSTRATIONS

ILLUSTRATIONS—Continued

TABLES

UNIT OF MEASURE ABBREVIATIONS USED IN THIS REPORT

°C	degree Celsius	in Hg	inch of mercury (atmospheric pressure)
dB	decibel	K	kelvin
deg	degree	kHz	kilohertz
ft	foot	ms	millisecond
ft/s	foot per second	s	second
h	hour	V	volt
in	inch		

CHARACTERISTICS OF ULTRASONIC RANGING SENSORS IN AN UNDERGROUND ENVIRONMENT

By W. H. Strickland[1] and R. H. King[2]

ABSTRACT

Ultrasonic ranging sensors are inexpensive, have no moving parts, have no lenses to clean, are normally small and unobtrusive, and can measure distances through moderate amounts of dust, smoke, and humidity, so they are well suited to underground mines. In the work reported here, conducted by the U.S. Bureau of Mines, researchers tested ultrasonic ranging sensors for their ability to define rib line features for computer-aided navigation of underground mine mobile equipment. The investigation began with laboratory tests of field of view, angle of incidence, intersensor variation, and ranging accuracy of the individual rangers in a ring array produced by Denning Robotics of Wilmington, MA. The results showed that the sensors have good accuracy and low variability.

Additional experiments at AMAX's Henderson Mine showed the sensors could accurately and reliably measure the distance to mine features, including convex and concave corners and rib intersections. The results showed that when used properly, the ranger data are accurate enough for reliable mine vehicle navigation.

When used incorrectly, ultrasonic rangers do not provide the anticipated data. Therefore, this report explains the principles of ultrasonic range measurement, describes the ranger's strengths and weaknesses, and explains proper ranger use and data analysis.

[1]Mining engineer, Pittsburgh Research Center, U.S. Bureau of Mines, Pittsburgh, PA (now manager, Experimental Mine, Colorado School of Mines, Golden, CO).

[2]Mining engineer, Pittsburgh Research Center; professor of mining engineering, Colorado School of Mines, Golden, CO.

INTRODUCTION

STATEMENT OF PROBLEM

Computer-aided vehicle guidance requires sensor data to relate the vehicle path to the desired trajectory and to identify obstacles that the vehicle must avoid. In an underground mine, the trajectory is projected based on targets or a digital map, unless the machine is excavating new territory. Consequently, sensor data are necessary to relate the vehicle's path and position to digital maps of mine features. An appropriate set of features to identify a vehicle's location are those present in the ribs: convex corners, concave corners, intersections, and roughly linear planes. Obstacles to be identified might include equipment, rocks from roof and rib falls, or personnel. The problem is to find a reliable and suitable sensor or array of sensors that locate the machine in relation to a wide range of objects using range data or other information.

Several imaging sensors, such as scanning laser rangers, stereo vision, and swept focus video, can accomplish this task; however, their purchase cost, maintainability, reliability, and computing power requirements make them difficult to apply in the mining environment. Some sensor systems, such as lasers and microwaves, are not readily accepted by work forces because of suspected health hazards.

Ultrasonic rangers are an attractive alternative because they are simple, durable, relatively inexpensive, and accepted by the people working near them. An initial demonstration using ultrasonic rangers to guide Carnegie Mellon University's Terregator mobile robot through an underground mine showed rangers have promise for use in mines (1).[3] However, ultrasonic rangers have not been characterized carefully for guidance of underground mining mobile equipment. These sensors have, however, been used widely at mines for bin level monitoring, and underwater sonar use has been well studied (2-3). Ultrasonic rangers have also provided data for laboratory mobile robot guidance (4-9). This study was part of the U.S. Bureau of Mines computer-assisted mining program to improve miner safety.

SCOPE

The research reported here attempts to determine whether ultrasonic range data can meet some of the navigation requirements of a computer-aided mining vehicle by clearly identifying mine features such as linear ribs, convex corners, and concave corners. The equipment used for these experiments was an array of 24 Polaroid[4] ultrasonic rangers mounted at 15° intervals around a 27-in fiberglass ring (made by Denning Mobile Robotics) interfaced with a microcomputer for data collection and storage (10).

Researchers designed the experimental procedures to test the ability of ultrasonic rangers to identify and define the common navigation features found in an underground mine. Laboratory tests established operating characteristics such as field-of-view (FOV) and ranging accuracy before underground tests began. The underground tests were designed to evaluate the ability of the sensors to delineate normal mine features such as corners, intersections, and ribs. Experimental data were collected at AMAX's Henderson Mine near Empire, CO (11). The rib feature was first surveyed using standard techniques, then the ultrasonic range data were collected. The range data were analyzed by comparing them to the rib outline as surveyed. Researchers mounted sensors on actual underground production load-haul-dump (LHD) units. This lead to a series of laboratory experiments on sensor covers or faceplates to improve durability.

RESULTS

This study showed ultrasonic ranging is a valid method for machine navigation. The rangers outlined convex and concave corners, ribs, and intersections. The rock and shotcrete surfaces in the underground mine normally cause a diffuse echo, so at least some of the sound wave returns to the sensor even at high angles of incidence. Accurate range readings were obtained up to a 60° angle of incidence.

A thorough knowledge of the task requirements, as well as the ranger's individual characteristics, is important. When used incorrectly, the rangers do not provide reliable data. For example, the ranger's FOV should be considered when analyzing range data.

---

[4]Reference to specific products does not imply endorsement by the U.S. Bureau of Mines.

---

[3]Italic numbers in parentheses refer to items in the list of references preceding the appendix at the end of this report.

ACKNOWLEDGMENTS

PRINCIPLES OF ULTRASONIC RANGE MEASUREMENT

Ultrasound frequencies are above the range of human hearing. The use of sound for ranging was developed in Europe just after World War I and was further refined during World War II (12-13). Underwater sonar ranging generally uses sound in the audio frequency range, the frequencies in the normal hearing range, but atmospheric ranging has usually been done with ultrasonic frequencies.

Ultrasonic rangers are transponders, that is, they act as transmitters by converting electrical energy into sound energy, then change roles to act as detectors (microphones) and convert sound energy into electrical energy. Two types of ultrasonic ranging transducers are commonly used for ranging in air: electrostatic and piezoelectric. A piezoelectric transducer impresses an ac voltage on a crystal, which vibrates and transmits a sonic pulse. While piezoelectric transducers couple very well to solids and liquids, they transmit only a small percentage of their energy to air.

Electrostatic transducers operate by causing a metallic-coated plastic film to vibrate at the same frequency as an applied voltage. They couple well to air because they have a large displacement amplitude (they vibrate with a great deal of intensity), which is needed to couple efficiently to low-density media that have high compressibility (media such as the atmosphere) (13).

Ultrasonic rangers transmit short bursts of high-frequency sound energy, commonly in the 13- to 60-kHz frequency range. The transmitted sound waves travel to an object, are reflected, and travel back to the sensor. Consequently, the distance can be calculated from the round trip time (time of flight) and the velocity of sound as shown in the following equation.

$$R = (V_a)(t/2),$$

where R = range (ft),

         V_a = velocity of sound (ft/s),

and t = round trip time (s).

The ultrasonic ranging transducer vibrates after the transmit wave has been sent out. This vibration can cause false range readings. To overcome this, most manufacturers have introduced a "blanking range." During this interval, the ranger is turned off and will not read any return signals. This blanking range is 0.0 to 0.9 ft for the rangers used in these experiments.

In most applications, the transducer is pulsed many times and the resulting ranges are averaged. The pulse rate of a ranger should be based on the range. The longer the range, the longer the ranger must remain in the receive mode, waiting for an echo, and the longer the required delay between transmit pulses.

VELOCITY OF SOUND

The velocity of sound at 20° C is 1,125 ft/s. Biber, Ellin, Shenk, and Stempeck (14) report that it changes only 0.35% over the maximum humidity change at 20° C and is virtually independent of pressure and elevation changes. However, temperature variation causes a 7% deviation from 0° to 40° C, because the velocity of sound changes with temperature of the air as described in the following equation:

$$V_a = V_o\sqrt{T/273}$$

where V_a = velocity of sound in air (ft/s),

         V_o = velocity of sound at 0° C (1,087.6 ft/s),

and T = temperature (K).

Ambient temperature sensor data can be fused with ranger data to correct the error, or the actual speed of sound can be measured over a known distance, and used to adjust the calculated range (16).

FIELD OF VIEW

An ultrasonic ranger can be treated as a plane, circular piston set in an infinite baffle. The radiated energy is conically symmetric about an axis perpendicular to the vibrating surface and passing through its center. That is, the ultrasonic ranging transducer consists of a plane surface that, at rest, lies flush with an acoustically hard wall. In operation it vibrates perpendicular to its surface and with constant velocity over its entire surface (17).

The acoustic field close to the ranger is very complicated (18). However, in the far field [distances greater than $D^2/(2\lambda)$], the spread of the acoustic beam depends on the ranger's diameter and wavelength as shown in the following equation (19):

$$\theta = 1.22\ (\lambda/D),$$

where θ =   acoustic beam angle in radians,

          λ =   wavelength,

and   D   =   ultrasonic ranger diameter.

The acoustic beam angle can be described as a contour drawn by connecting the points in space at which the energy by the ranger has dropped an equal level, for example, 3 or 6 dB (18). Researchers tested a 14-in-diameter, piezoelectric ultrasonic ranger operating at

13 kHz, made by Milltronics, that measured ranges up to 200 ft with 5.5° acoustic beam angle.

When measuring distance to an object, the beam geometry is important, but the surface characteristics of the object and the sensitivity of the ranger are equally important. The experiments reported herein measure the combination effect of these factors and consequently use the term "field of view" (FOV) instead of beam angle. The FOV is the beam angle at which an object with certain surface characteristics reflects enough sound to be detected by the ranger.

The sound energy radiation pattern from a ranger has many side lobes when the ranger's radius is large in comparison to the transmitted wavelength (18). The Polaroid ranger, with a 0.75-in radius and a wavelength of 0.27 in, produces a three-lobe pattern. In this research, the average FOV of the major, on-axis lobe is represented with the conical envelope shown in figure 1.

An acoustic sonar ray (vector OE in figure 2) is used to compare ranger and physical survey data in this report. The sonar ray is the center of the sound energy transmission. The angle of incidence (I) is the angle between a perpendicular-to-the-target surface and the sonar ray as shown in figure 3.

ATTENUATION

Because the transmitted ultrasonic energy wave spreads over an increasingly large area the farther it travels from
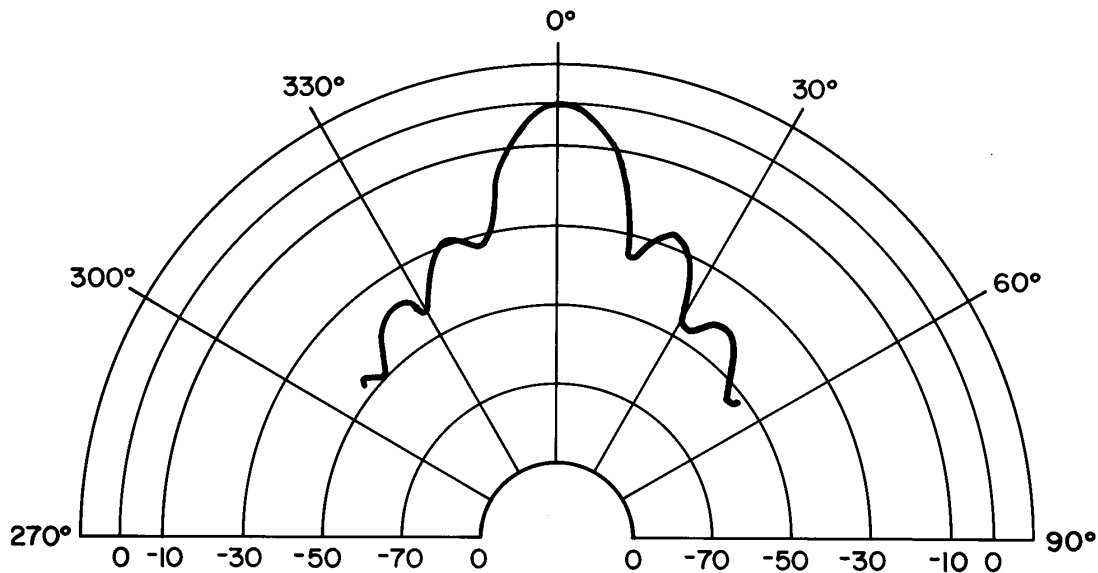

Figure 1.—Polaroid sound energy radiation pattern at 50 kHz (after Polaroid, 1982 (21)). Note: Decibels normalized to on-axis response.
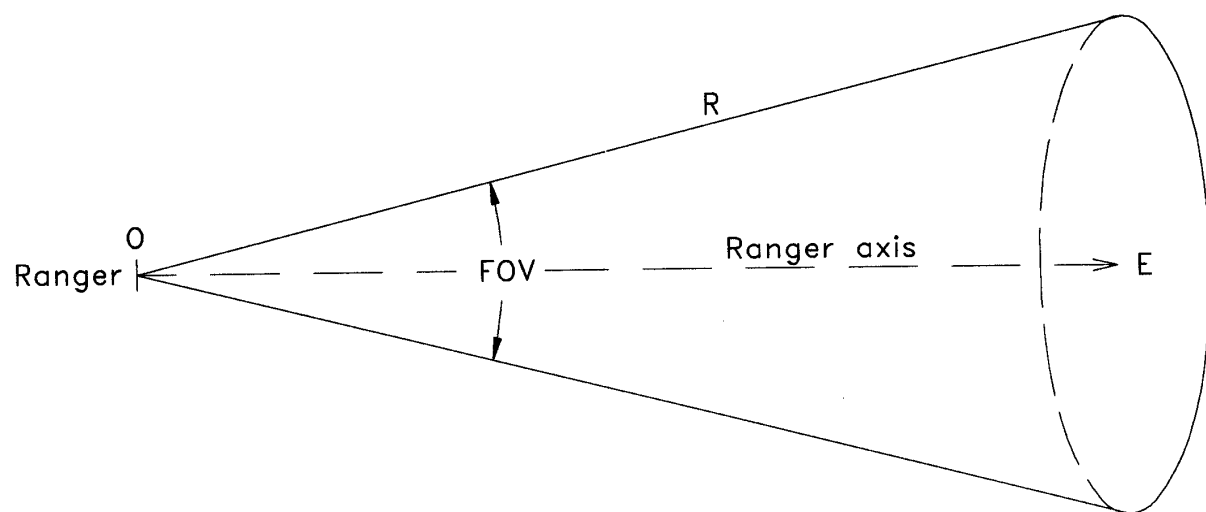
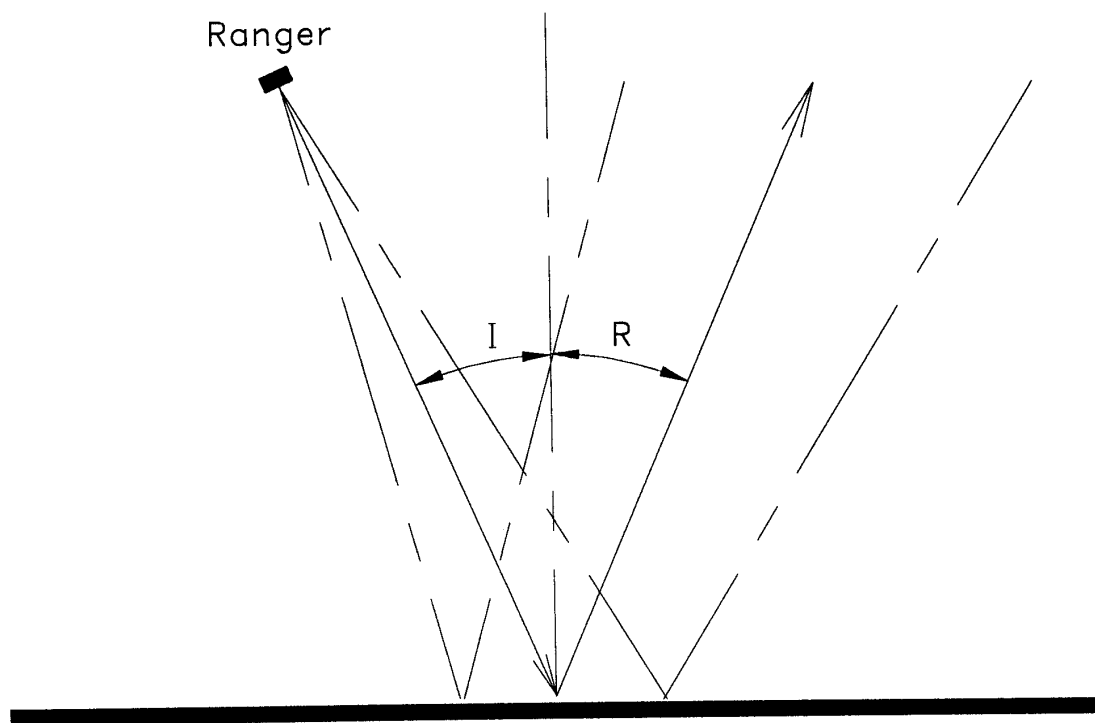**Figure 2.—Ultrasonic ranger's ideal field of view.**

Figure 3.—Angle of incidence. (I = angle of incidence, R = angle of reflection.)

the sensor, signal power decreases as $1/d^2$, where d is the distance traveled (14). The reflected signal strength is again reduced by a factor of $1/d^2$. In addition, there are viscous losses and heat conduction losses (classical absorption), and losses associated with molecular exchange of energy.

Viscous losses are similar to friction losses but occur during the expansion and compression of the air as the sound wave advances (18). The sound wave causes temperature variations that produce heat conduction losses. Heat transfers from the regions of higher temperature (the sound wave) to those of lower temperature (the atmosphere). Molecular losses occur during the collision of gas molecules as the sound wave travels. Energy transfers from the sound wave to the internal structure of the molecule (20).

Thus, the power of a sound wave transmitted in the atmosphere dissipates rapidly with distance according to the following equation (14):

$$P_r = [(e^{-2ad})/d^4]\cdot P_t,$$

where P_r = power of received signal,

P_t = power of transmitted signal,

a = absorption coefficient (atmospheric absorption per unit distance),

and   d = distance from the source.

SURFACE CHARACTERISTICS

The characteristics of the reflecting surface have a significant effect on the reflected signal. Some very smooth surfaces, such as polished metal, water, and sometimes a rock surface with water on it, reflect the sound without any significant scattering. This reflectivity causes problems if the angle of incidence is large, that is, if angle I in figure 3 is not close to 0°. At large angles the sound wave bounces away from the ranger (fig. 4). Consequently, only a small amount of sound reflects back to the
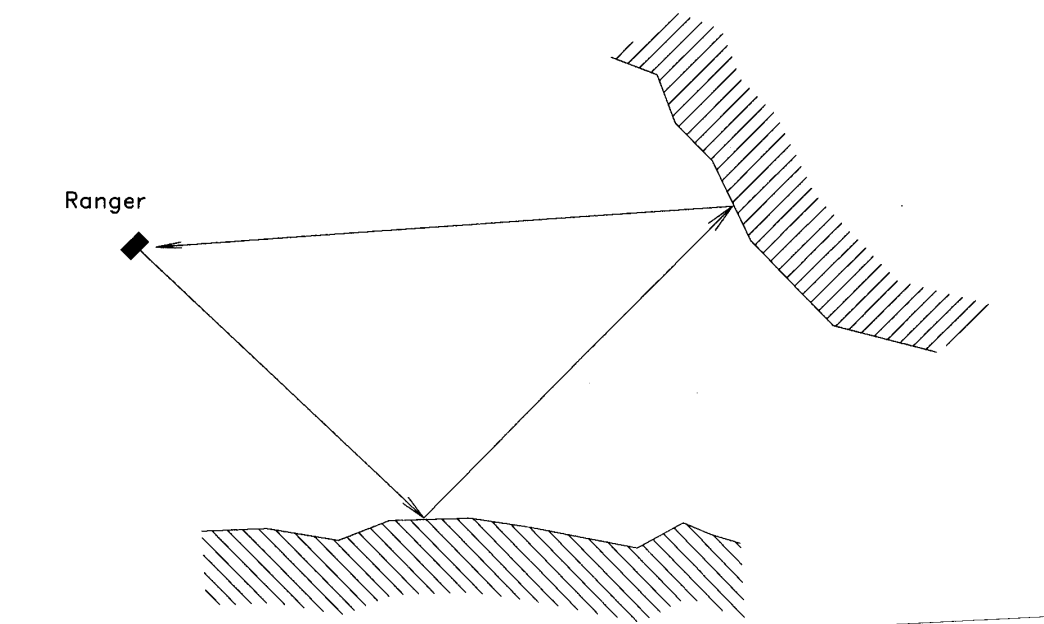

Figure 4.—Multiple reflections causing false range reading.

sensor and the reflection cannot be distinguished from the background noise.

The bounced sound wave may reflect from several surfaces before returning to the sensor, thus traveling over a longer path and causing an apparent return from an object at a more distant range (fig. 4). The surfaces encountered in these tests were rough and diffused the sound reflections, so this was not a problem.

Highly absorptive surfaces, such as plastic foam, may reflect so little sound at certain wavelengths that the return is too weak. Extremely smooth surfaces might produce reflections that interfere with the transmitted sound wave. The interference effect is wavelength dependent, so an echo that is weak at one frequency may be much stronger at another frequency. Consequently, Polaroid produces a ranger with a transmit burst composed of 60-, 57-, 53-, and 49.7-kHz waves (15).

RANGING ACCURACY

Ranging accuracy is greatly improved if the actual ambient speed of sound is used for all calculations. Inaccuracies can be introduced to the range readings by the length of the transmit burst; the surface characteristics of the target, as described previously; the detection threshold of the ranger; and the beam width.

The ultrasonic ranger reports the range to the very first object that produces an echo above the threshold point. There may be more than one object in the spreading acoustic beam. Therefore, the range reported may not be the range to the object being used to safely and accurately guide the machine.

The ranging circuitry normally starts timing for an echo the instant that it transmits a wave. If the transmit pulse is long and the target surface irregular, the last piece of the transmit may produce the only echo strong enough to trigger the ranger's threshold. It is difficult to determine which part of the transmit wave created the echo; therefore, the transmit burst should be kept as short as possible.

Other errors result from the method of echo amplification. The Polaroid ranger has a "step" amplification gain; the gain of the amplifier increases in discrete steps with time (14). If the increase in gain occurs in the midst of an echo, a false range reading may result.

THE POLAROID RANGER

The Polaroid ultrasonic ranger is an electrostatic transponder that transmits a pulse and then turns into a receiver (or microphone) (21). Figure 5 shows a typical transmit and receive pulse from the Polaroid ranger in the Denning ring array. The ranger precision is 0.1 ft over a 0.9- to 35.5-ft range, but rangers can be modified to obtain greater resolution over shorter ranges. The rangers used in this research measure from 0.9 to 25.5 ft.

In transmit mode, the sensor's components, a thin, sensitive foil composed of gold-coated polyester film stretched over an aluminum backplate (fig. 6), act as a capacitor. The foil vibrates at the impressed ac voltage frequency to emit sound energy.

Any echo received by the ranger also causes the foil to vibrate. The ranger now functions as a microphone and produces an ac that ranges from volts to microvolts depending on the echo signal strength. The farther an echo source is from the ranger and the more absorptive the echo object surface, the lower the echo's energy and the lower the amplitude of the voltage produced by the ranger. Therefore, amplification is required to distinguish low-strength echoes.

Researchers studied sources and amplitudes of internally and externally generated noise in the ranger circuit. Numerous waveforms captured at high-frequency sampling with a digital storage oscilloscope showed that the internal noise in the Polaroid ranger's circuitry is minimal. The frequency of 49.7 kHz, used in the Polaroid sensors tested, was above that measured on diesel-powered mining equipment, so there were no interference problems from external sources (22). However, additional testing is necessary before using lower frequency sonic rangers.

The Polaroid ranger differentiates between a legitimate reflection and noise by assuming the reflection amplitude will exceed a constant threshold. The first echo that exceeds the threshold is used to determine a range reading. The object that produced this echo may or may not be the object of interest. For example, the objective of this research was to measure distance to rib features. Sometimes, the sensor reported distance to small objects such as wires or protruding bolts that reflected enough sound to trigger the ranger. Some manufacturers, such as Milltronics, incorporate programmable processors with the ranging system to solve this problem.
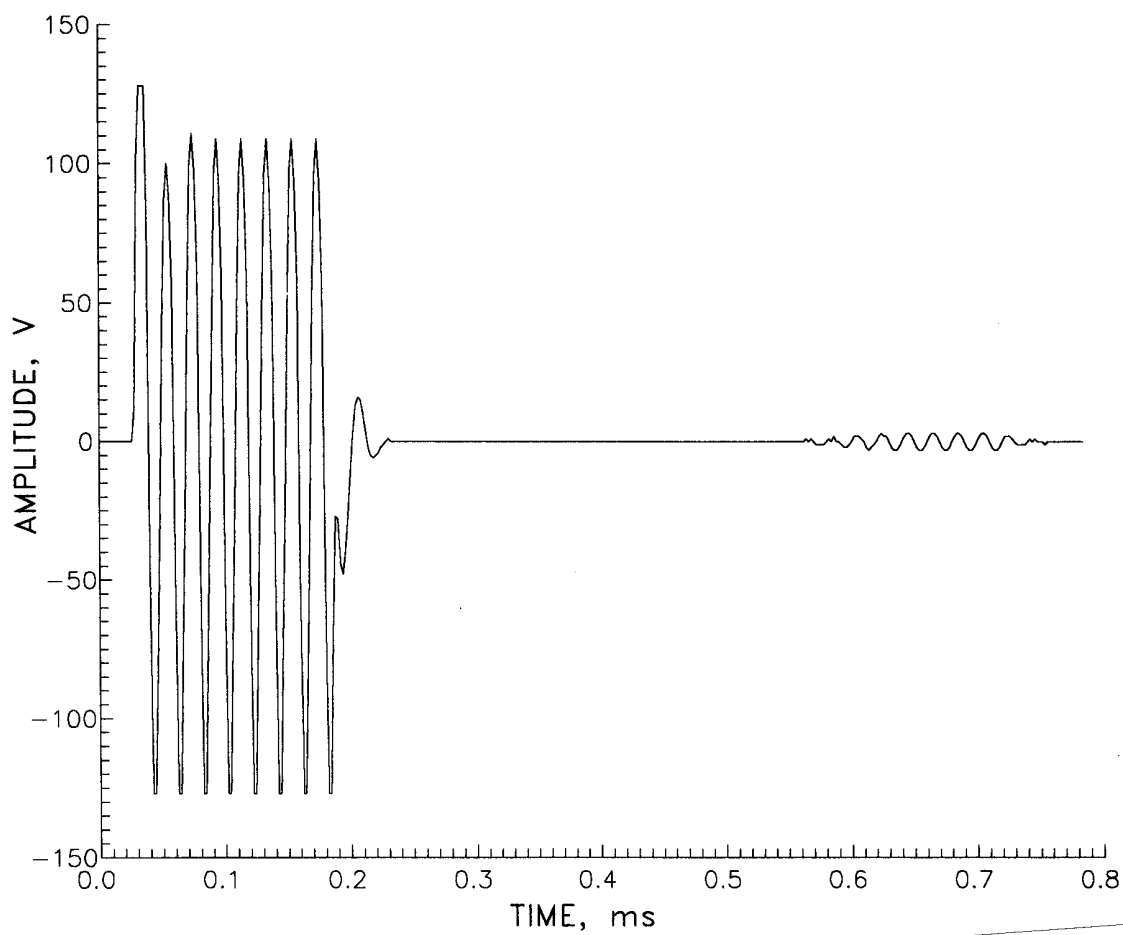
Figure 5.—Sample of transmit and receive pulse from Polaroid ranger as used in Denning ring.
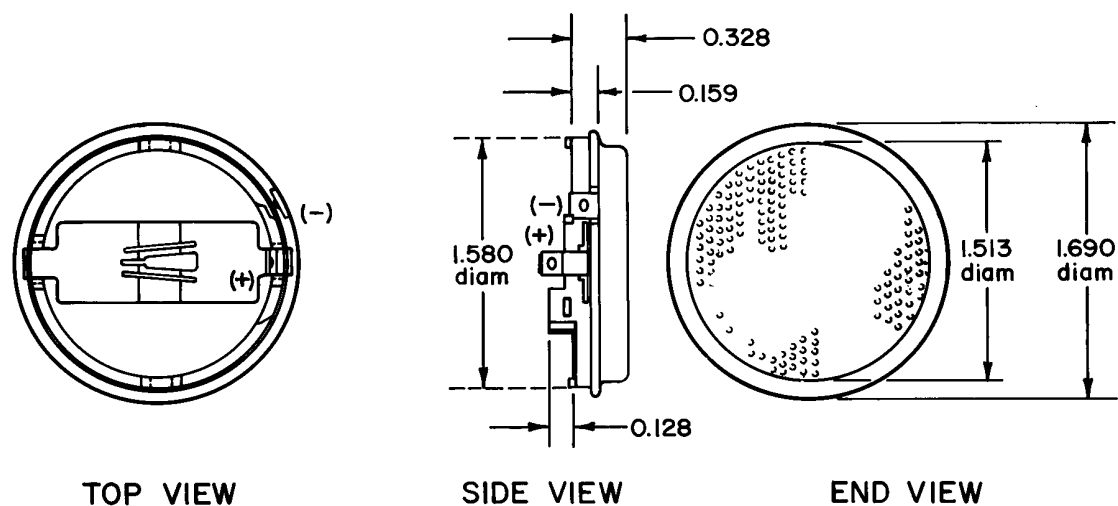

TOP VIEW   SIDE VIEW   END VIEW

Figure 6.—Polaroid Instrument Grade Ranger (after Polaroid, 1982 (21)). Dimensions are in inches.

CHARACTERIZATION OF ULTRASONIC RANGERS

Before an ultrasonic ranger can be used for machine guidance, the operating characteristics of the specific ranger must be tested within the environment in which it will be used. This research started with laboratory tests, and later moved underground.

LABORATORY TESTS

A series of laboratory experiments characterized the sensors before underground tests began. The equipment used for most of these experiments was an array of 24 Polaroid ultrasonic rangers mounted at 15° intervals around a 27-in fiberglass ring, shown in figure 7. Denning Mobile Robotics, Inc., of Wilmington, MA, developed the ring and its control processor. Figure 7 also shows a microcomputer interfaced to the ring through the RS-232 port to collect and store range data.

Interference between the rangers is prevented by pulsing each sequentially with a user-selected time delay of 18 to 250 ms between transmit bursts. The user can also select the sensors to be fired, and the firing sequence. For example, the controller can fire all sensors (0-23) in numerical order, or only fire three rangers in the sequence 0, 8, 16. The controller can repeat the previous sequence, or change it to another, say 1, 9, 17, for the next sequence. This allows the user to select only those sensors needed for the experiment, and prevents the transmit pulse of one sensor from interfering with the received signal of another sensor.

Laboratory tests evaluated range resolution, intersensor variation, and FOV by moving a 1.5- by 2.5-ft rectangular cardboard target and a 3/4-in by 4-ft wooden dowel to different locations within the FOV of sensor 0. When measurements were completed on sensor 0, the ring was rotated 15° and the experiment was repeated for sensor 1, 2, and so on, until eight sensors were tested. Researchers stored range data sets from each of eight sensors at 2.5, 5, 7.5, 10, 12.5, 15, 20, and 25 ft.

Table 1 shows good resolution and little intersensor variation up to 7.5 ft. From 10 to 20 ft the readings varied from the measured distance by as much as 0.2 ft. Variation among the sensors, however, was less than 0.1 ft. The target did not reflect enough sound energy to be detected at longer ranges.

Researchers moved the targets at right angles to the sensor axis and across the FOV (fig. 8) to define the extent of the FOV. The FOV was 17.6° (8.8° on either side of the sensor axis) at a range of 5 ft. The sound energy is highest close to the ranger and along the sensor axis. The wave is weakest near the edges of the FOV; consequently, the FOV appeared to decrease to 13.8° at 10 ft, and 10.6°

at 15 ft, because of the weak echo when the target was on the edges of the 17.6° FOV.

Table 1.—Accuracy of range readings for sensors 0 to 7 used in Denning ring segment, feet

(Temp, 28° C; humidity, 48%; elev, 5,775 ft; pressure, 24.50 in Hg)

Measured distance to box	0	1	2	3	4	5	6	7
2.5	2.5	2.6	2.5	2.5	2.5	2.5	2.5	2.5
5.0	4.9	5.0	5.0	5.0	5.0	5.0	5.0	5.0
7.5	7.5	7.5	7.5	7.5	7.5	7.5	7.5	7.5
10.0	9.9	10.0	9.9	9.9	9.9	9.9	10.0	9.9
12.5	12.4	12.4	12.4	12.4	12.4	12.4	12.4	12.4
15.0	14.8	14.9	14.8	14.8	14.8	14.9	14.9	14.8
20.0	19.8	19.9	19.8	19.8	19.8	19.8	19.9	19.8

To further investigate the effect of an object's surface characteristics on FOV, researchers moved a vertically mounted 3/4-in wooden dowel, tall enough to intersect the entire FOV horizontally, across the FOV. The use of a nonplanar object reduces the effects of incidence angle on the FOV. The dowel tests produced a 22° average FOV at 5 ft, 15.3° at 10 ft, and 12.6° at 15 ft. The increase in the FOV over the cardboard target was caused by the dowel's more diffuse scattering of the sound wave over a wide angle. Although the echo was weak, at least some of the energy reached the ranger. The cardboard echo was not diffused and probably reflected along a line that missed the ranger. In addition, cardboard absorbs more sound energy than smooth wood.

UNDERGROUND MINE EXPERIMENTS

The Denning ring was tested at AMAX's Henderson Mine near Empire, CO, after the sensors had been characterized in the lab. Three types of underground navigation features were defined, consistent with Kuc and Siegel's corner-edge-wall navigation model: concave corner, convex corner, and linear rib (fig. 9) (23).

Linear Rib Experiment

The experiment began with choosing a section of straight rib, surveying it with traditional techniques, and producing the contour map of figure 10 showing the surface characteristics. The Denning ring was then placed on a platform 4.25 ft above the floor (fig. 11) and approximately 5 ft from a straight section of the rib. The sensor axes aligned with the 18-in line shown on the vertical axis of the figure 10 map.
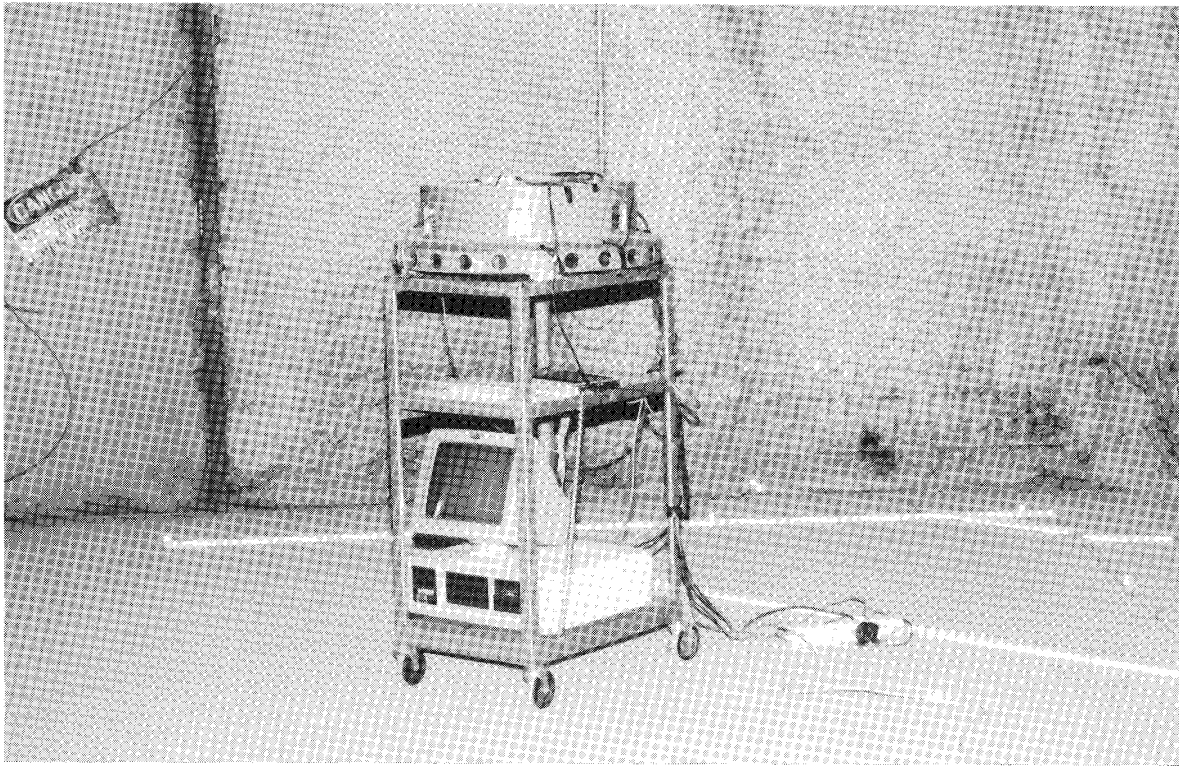
Figure 7.—Denning ring and microcomputer.

Ranger

Ranger axis

KEY

● Target detection point

0 1 2 3 4 5
Scale, ft
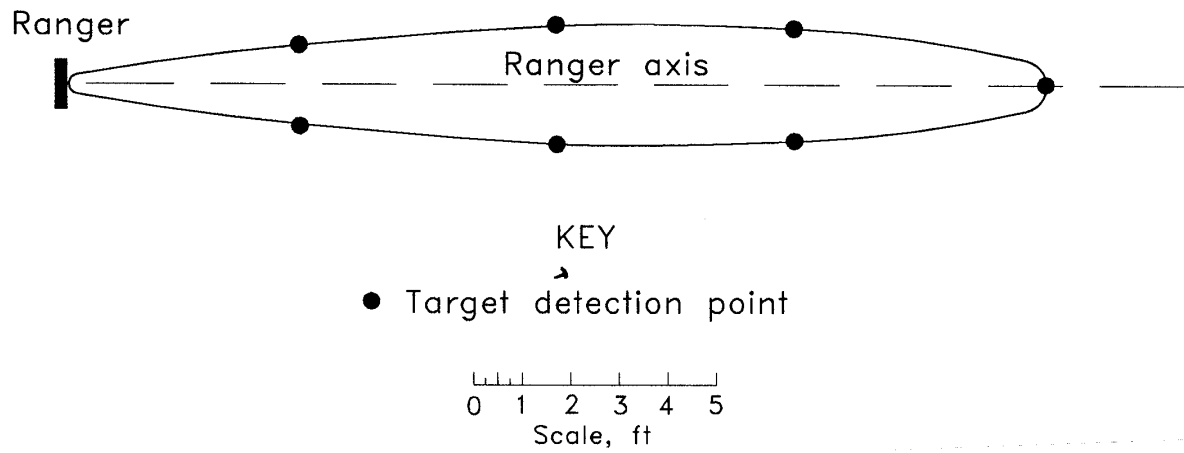
Figure 8.—Field of view test.

Concave corner   Convex corner

Wall

Figure 9.—Mine navigation features.

Figure 10.—Contour map of rib surface (contour interval = 2 in). Sensor axes were located at y = 18.
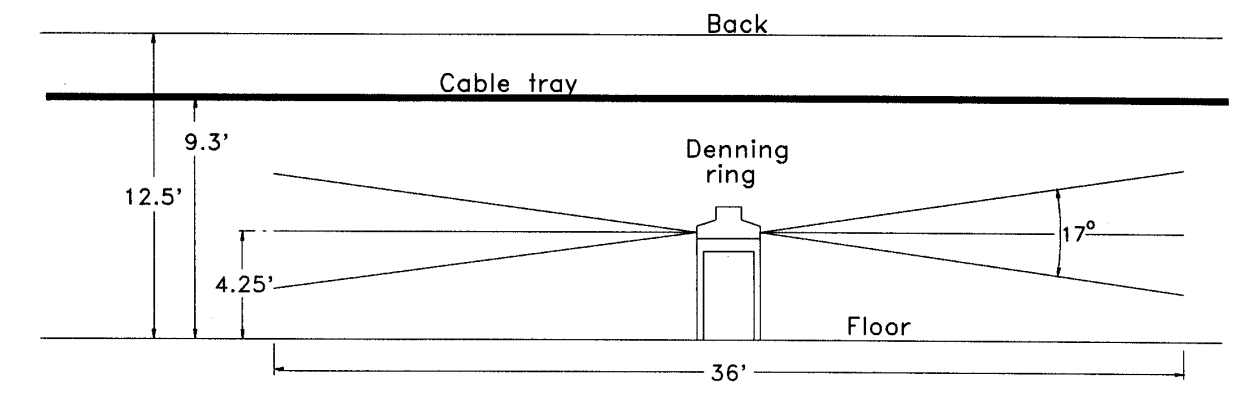
Figure 11.—Side view of Denning ring in linear rib experiment.

Researchers rotated the ring through 105°, stopping at each 5° increment to gather range data. Figure 12 shows the rib as surveyed along with the position of the ring, and sonar rays to the range reading. The mode of 10 range readings was used to produce the drawings shown. The range readings from the sensors produced a very good, though not exact, delineation of the rib.

The modes, in feet, of 10 range readings at 0° angle of incidence, listing ranging accuracy to mine rib at a distance of 5 ft, follow: sensor 0, 4.8; sensor 1, 4.8; sensor 2, 4.8; sensor 3, 4.9; sensor 4, 4.9; sensor 5, 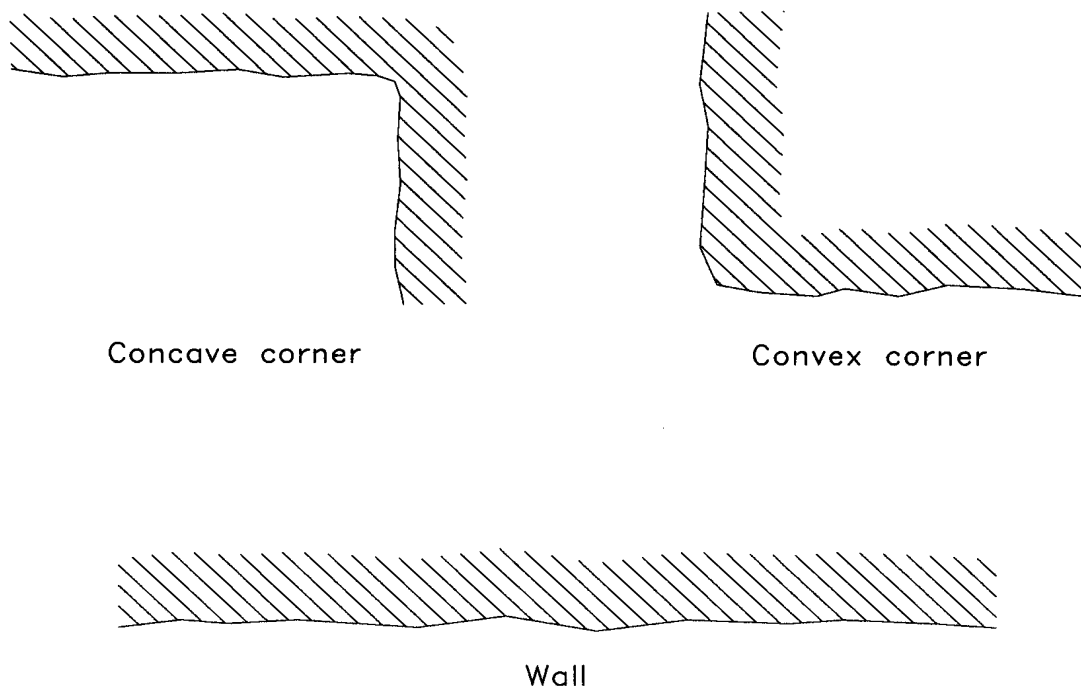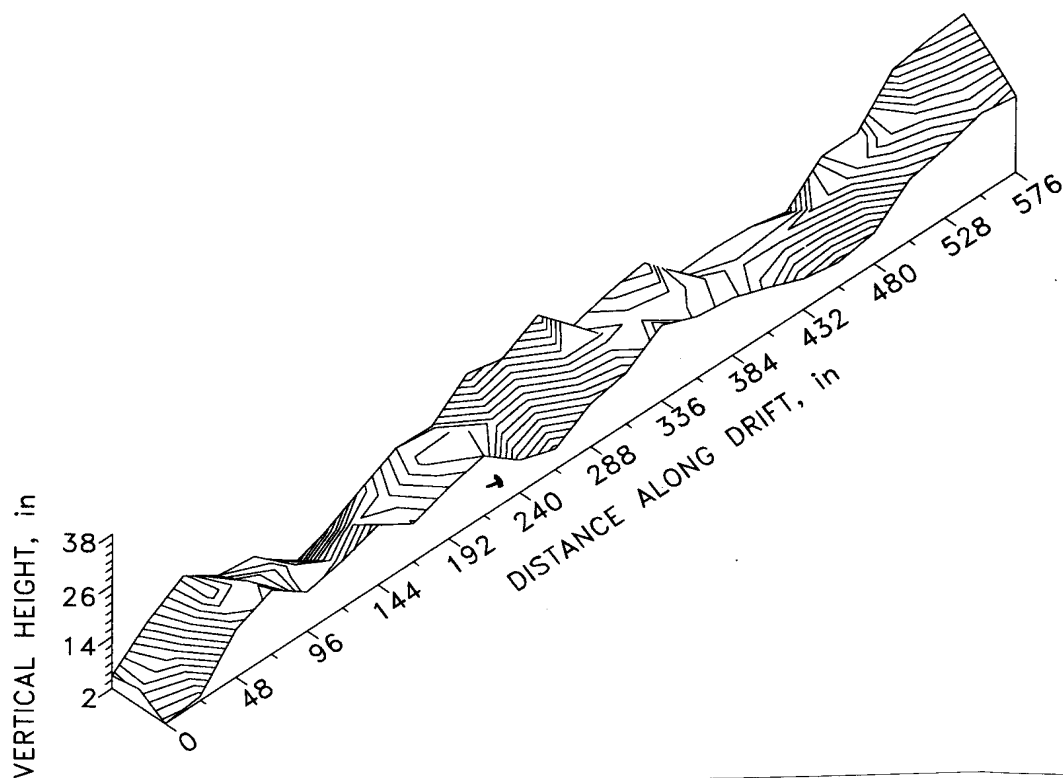4.9; sensor 6, 4.9; sensor 7, 5.0. Temperature was 28° C, humidity 54%, elevation 7,500 ft, and pressure 22.71 in Hg. The resolution compares favorably with that found in the laboratory experiments. Intersensor variation was quite a bit higher, however, with range readings varying by as much as 0.2 ft at a measured range of 5 ft. Misalignment of the sensors in their ring mountings contributed to this variance. In addition, each sensor's FOV enveloped different rib features, causing variations in range readings.

Angle of incidence to a rough mine rib is an important measurement. If reliable data cannot be obtained at high enough incidence angles, sensors on the front of a computer-aided machine will not be able to define the rib lines far enough ahead for reliable trajectory generation. At 60° incidence, range readings defined the rib with adequate precision (a maximum error in this experiment of 9 in). Sixty degrees is probably adequate for mine vehicle guidance.

Borenstein and Koren (24) determined 25° was the maximum angle of incidence for a "smooth" surface. The rangers detected the mine rib at angles greater than 60° (0° being perpendicular to the rib), but the data varied too much. The variability results from rib protrusions

intersecting the FOV, which produces weak reflections that intermittently exceed the ranger's amplitude threshold.

As the rangers were oriented parallel to the drift centerline, they did not measure the expected maximum distance of 25.5 ft. Instead, they sometimes received an echo from the floor, the back, or the overhead cable tray because the transponders were misaligned in the ring. This problem was not a fault of the rangers, but was probably due to their mounting.

Concave Corner

Next, researchers determined the ability of the rangers to define concave corners by using traditional surveying techniques to develop a rib baseline, setting the ring and computer on a cart as shown in figure 7, and then mapping the ribs with the ultrasonic rangers for comparison. The ribs were rough surfaces with numerous large, angular features, similar to the linear rib, created by drill-blast-muck operations. The wall between the ribs was shotcrete sprayed on plywood (fig. 7).

The cart was moved along a set of four approach lines parallel to the ribs, shown in figures 13 through 16, and along the diagonal approach path shown in figures 17 through 19, stopping every 2 ft for data storage. The sensor 7 axis paralleled the approach paths, and the diagonal approach line was midway between sensors 3 and 4. The figures show the sonar ray to the most frequently occurring (mode) range reading, superimposed on the surveyed rib edges.

The results show that in the diagonal approach experiment, the sensor array clearly defined the concave corner. However, the rangers could not see all the way into the corner in the parallel approach experiments. This
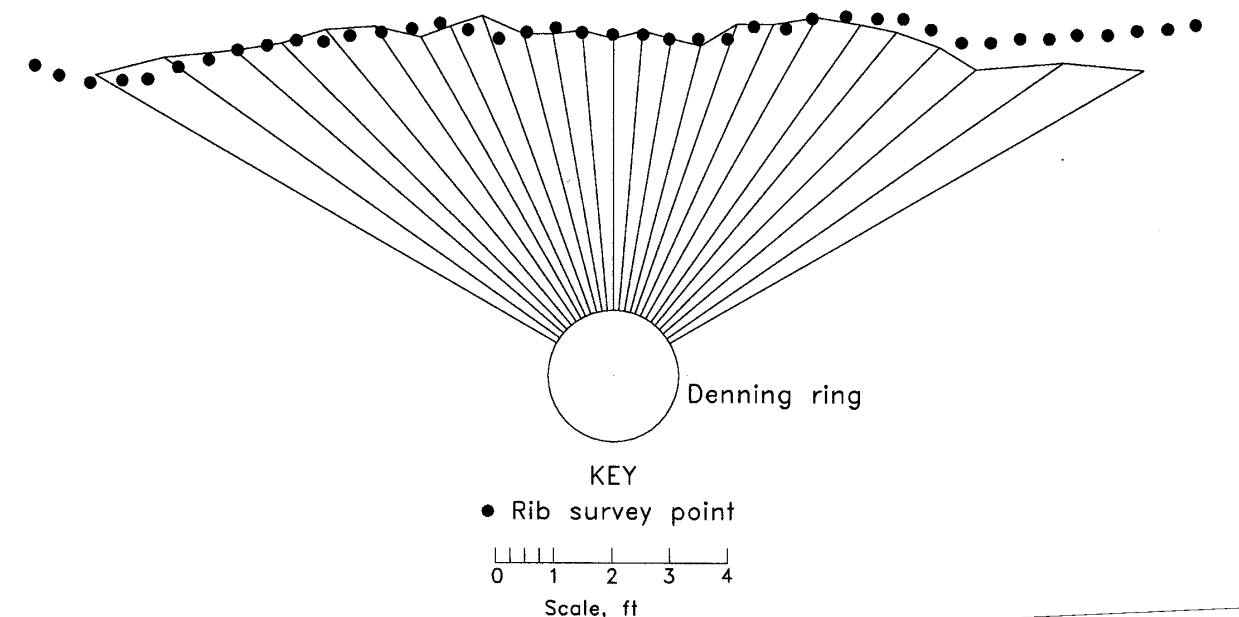
KEY

● Rib survey point

```
L I I I L___I___I___J
0   1   2   3   4
```

Scale, ft

Figure 12.—Sonar ray representation of rib versus surveyed rib.

phenomena may be explained by the sides of the sound energy radiation pattern echoing from rib protrusions.

Convex Corner

Next, researchers surveyed and mapped a convex corner (fig. 20) and then moved the cart-mounted sonar ring along the approach lines shown in figure 21, again stopping every 2 ft to collect data. The sensor 0 centerline aligned with the 0°, 45°, and 90° headings, and the sensor 4 centerline aligned along the 135° heading.

Figures 22 through 26 show the results of the 0°, 45°, and 90° tests. The data did not describe the corner with perfect precision, but the data from most approach angles should be adequate for computer-aided machine guidance, because it closely describes the shape and location of the corner.

The ranger FOV and incidence angle are key factors in defining a corner like this. When an ultrasonic ranger approaches a convex corner, the reflecting walls are effectively turning away from the sensor axis. But the edges of the sensor FOV are still identifying an occupied region and suggesting a wall of some type. If more precise data are necessary for high-speed machine guidance, data corrections can be attempted by recognizing patterns in the echo waveform. King and Gordon (25) recognized objects

in ultrasonic transducer echoes with pattern recognition algorithms. King believes the FOV edge reflection shape will be significantly different from an echo reflected from an object located more centrally in the FOV.

Figures 27 and 28 show the data from the 135° approach at 6 and 14 ft. The range readings from the sensor ring do not define the corner very well at this approach angle. As the rib turned away from the ranger, the edges of the ranger's FOV echoed from protrusions or angled surfaces on the actual mine rib.

Even though sensor 4 moved toward the corner in precisely 2-ft increments, the tabular data show different results. The narrowing of corner (the intersection of the two ribs), the fact that the corner was not perpendicular to the central ray of the sensor, and the fact that the area viewed by the sensor decreased as it moved toward the corner all contributed to this unexpected result.

Intersection

The ability of the rangers to represent a drift intersection was first determined by placing the ring on a track-mounted push cart, moving through the intersection, and stopping to collect data in 2-ft increments. The sensor 7 axis aligned with the direction of travel; consequently, the sensor 1 axis was perpendicular to the rib.

Shotcrete wall

Rib

Rib

A   B   C   D

KEY

—— —— Approach line

0   1   2   3   4
Scale, ft
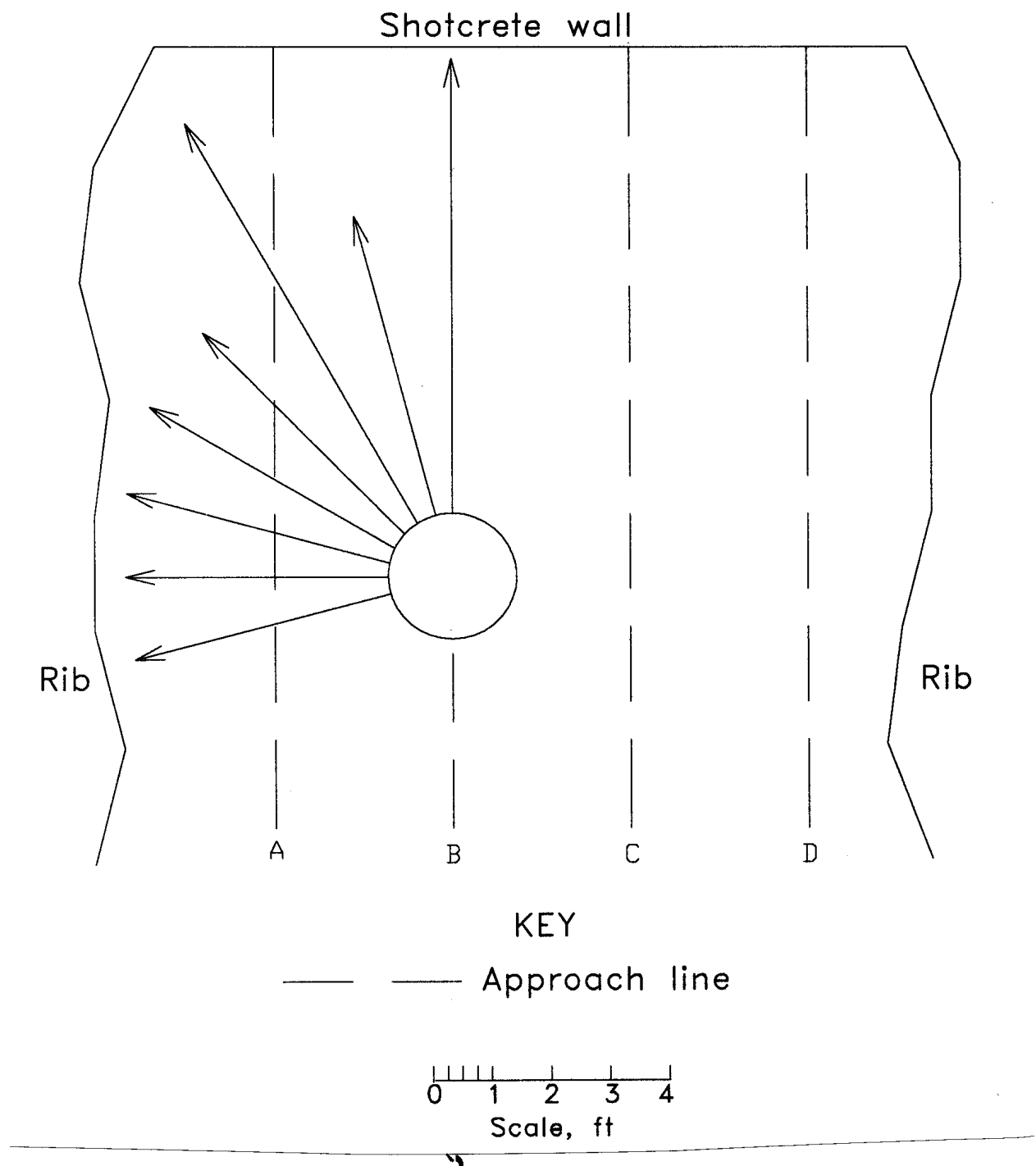
Figure 13.—Parallel approach to concave corner, path B, about 8 ft away.

Shotcrete wall

Rib

Rib

A   B   C   D

KEY

—— —— Approach line

0   1   2   3   4
Scale, ft
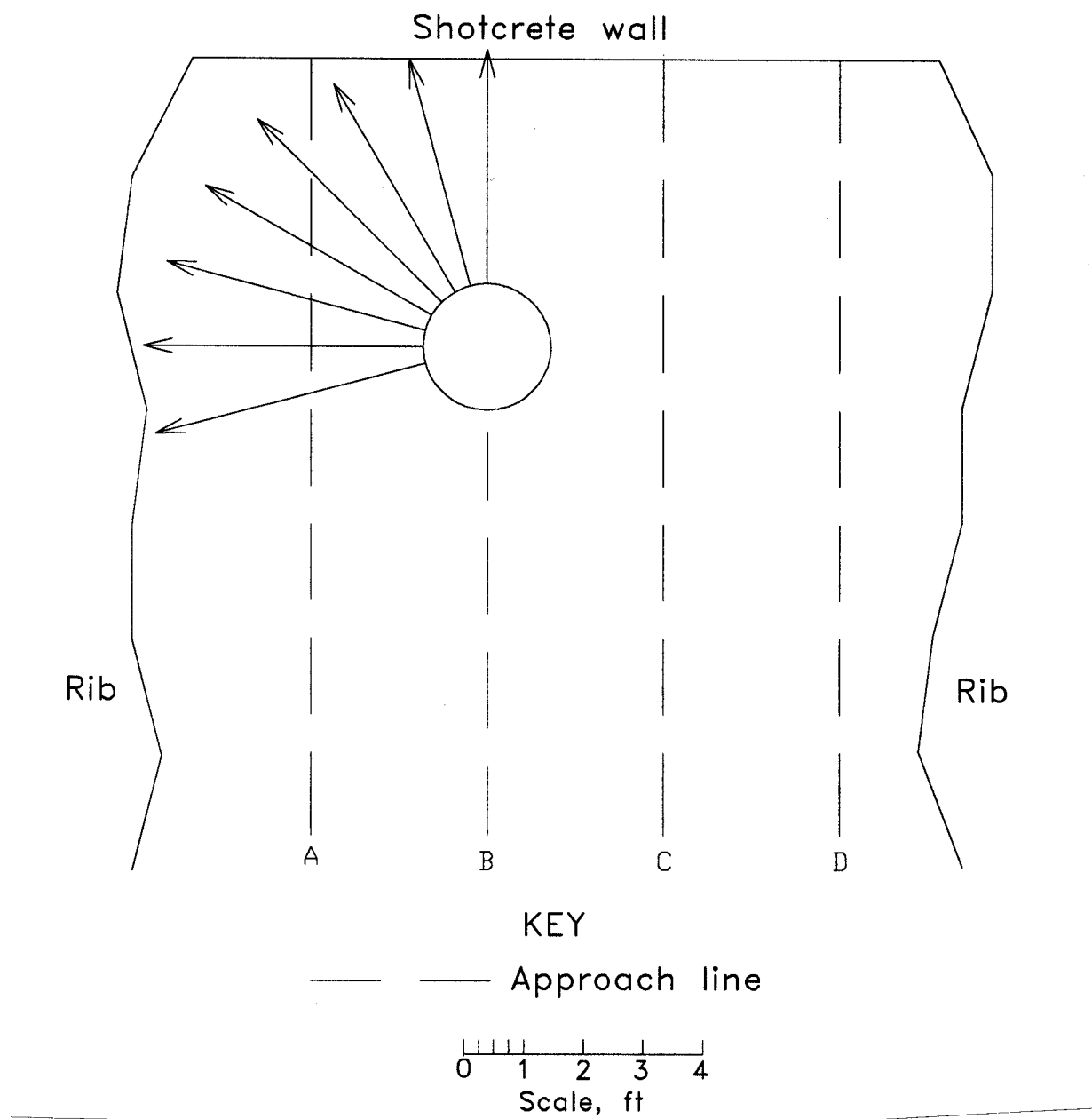
Figure 14.—Parallel approach to concave corner, path B, about 4 ft away.

Shotcrete wall

Rib

Rib

A   B   C   D

KEY

———   ——— Approach line

0   1   2   3   4
Scale, ft
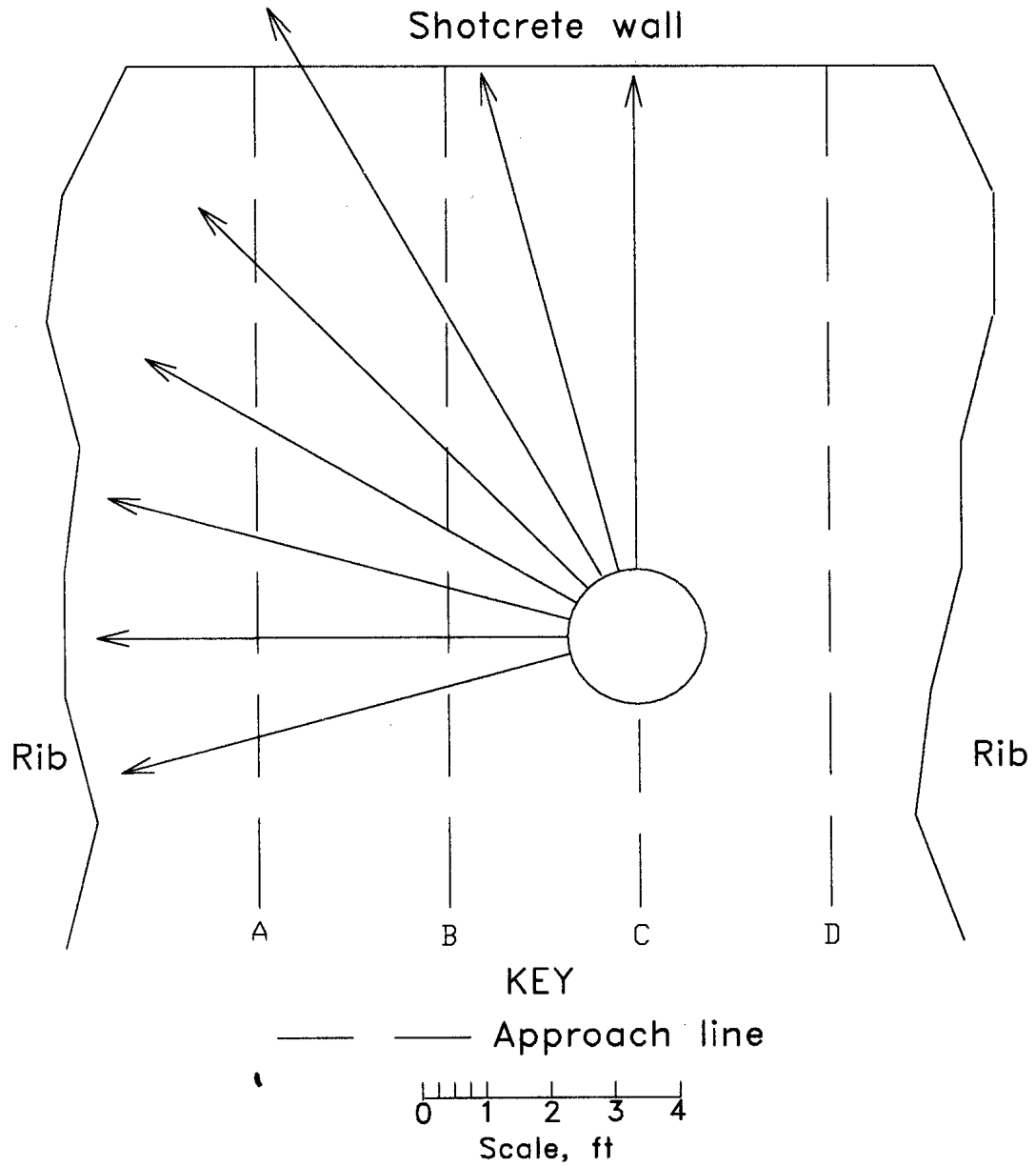
Figure 15.—Parallel approach to concave corner, path C, about 8 ft away.

Shotcrete wall

Rib

Rib

A   B   C   D

KEY

—————— Approach line

0   1   2   3   4
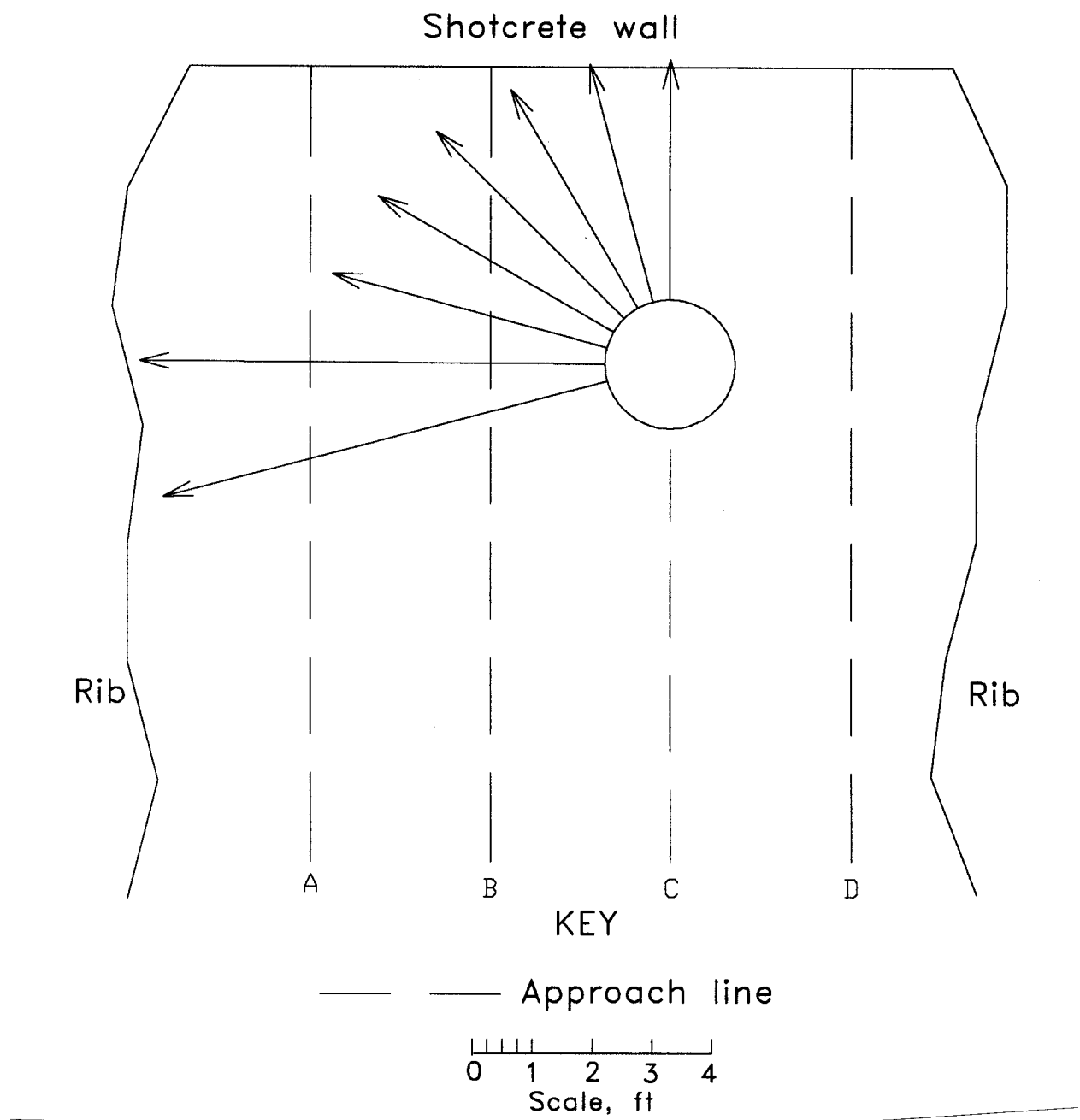
Scale, ft

Figure 16.—Parallel approach to concave corner, path C, about 4 ft away.

Shotcrete wall

Frame

Rib

KEY

———— ———— Approach line

0 1 2 ` 3 4 5
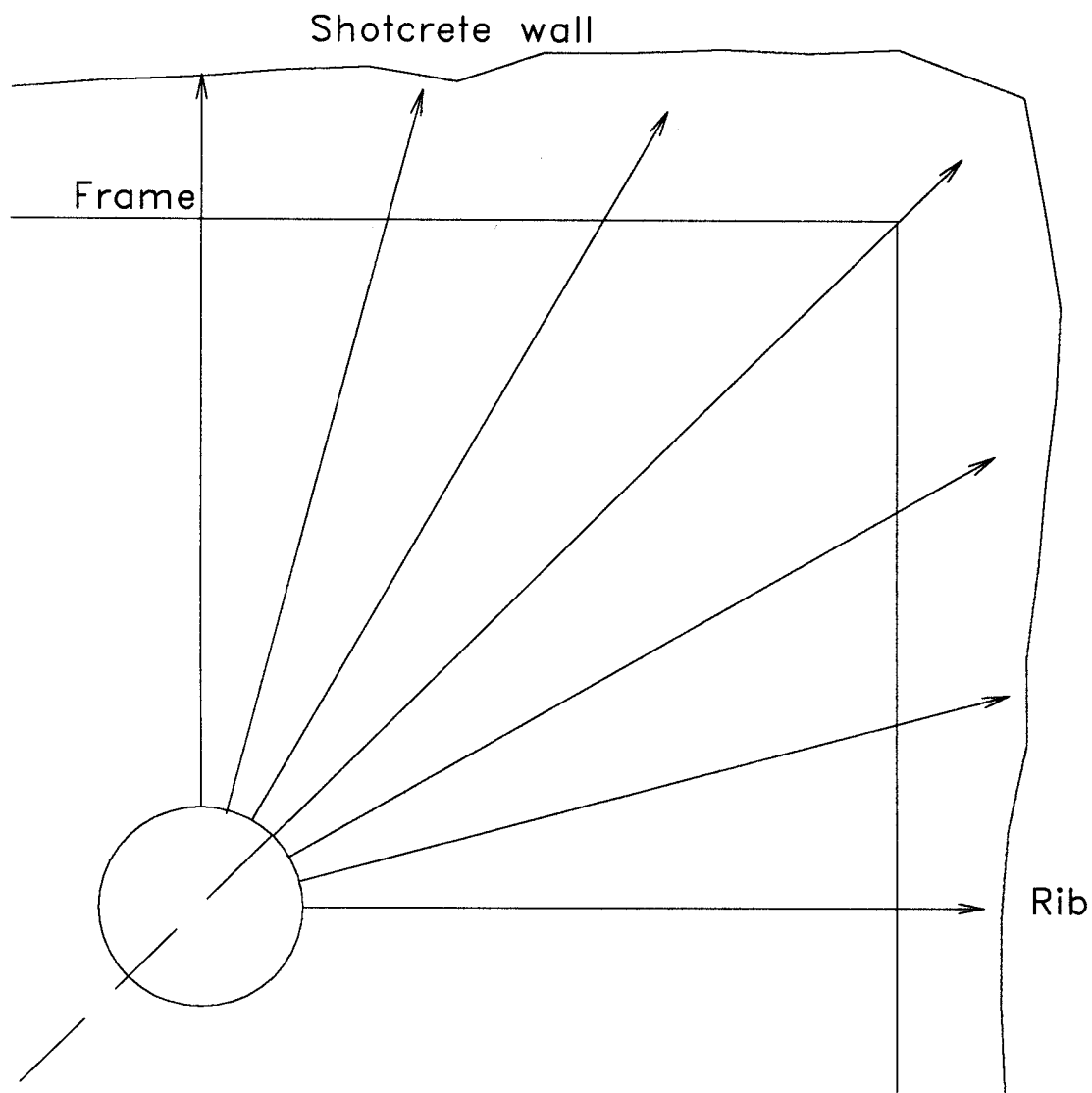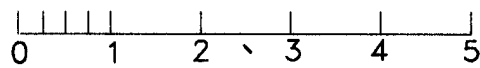
Scale, ft

Figure 17.—Surveyed concave corner rib and range readings at 10-ft setup.

Shotcrete wall

Frame

Rib

KEY

———— ———— Approach line

|_|_|_|_|_| | | | |
0   1   2   3   4   5

Scale, ft
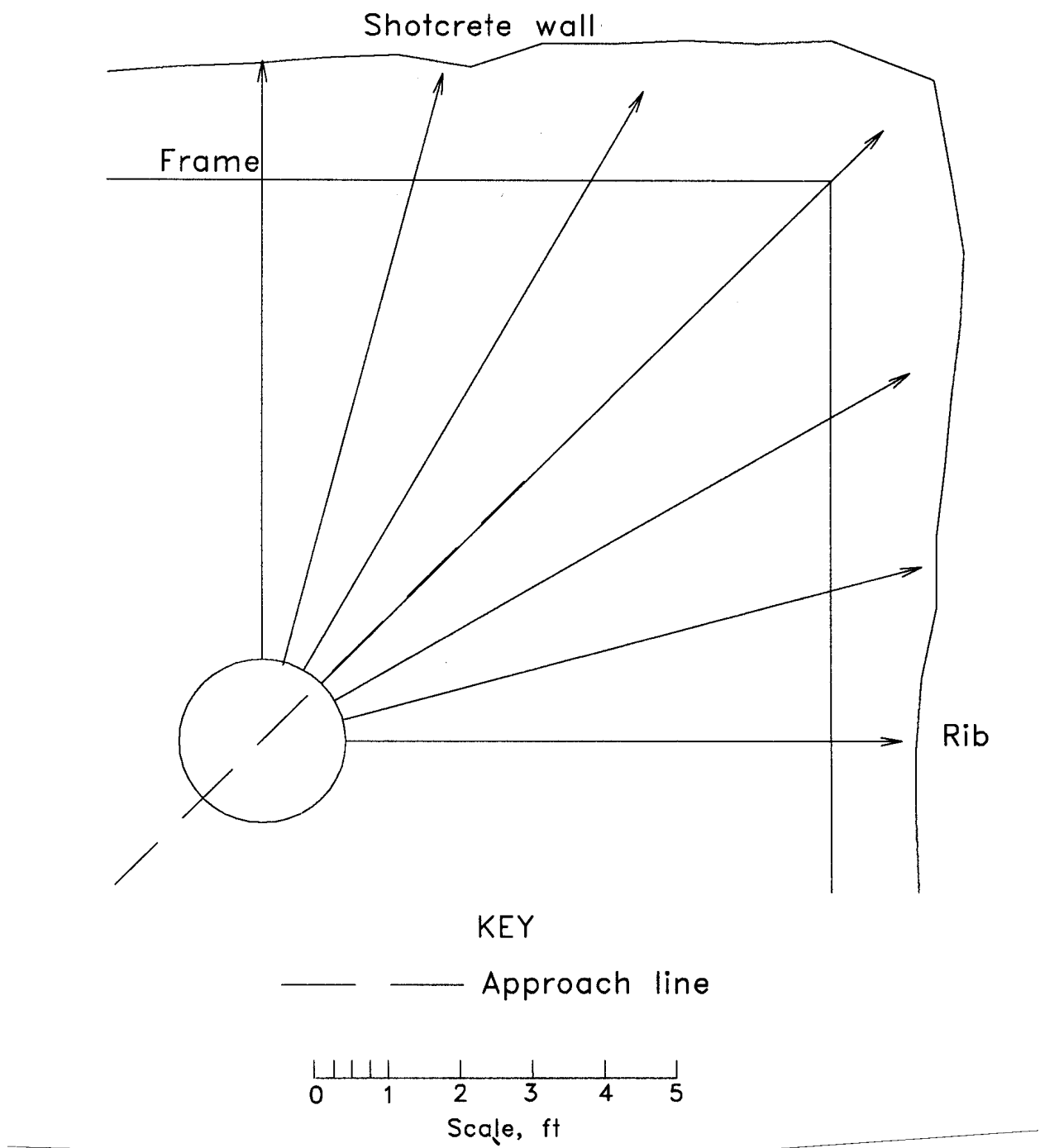
Figure 18.—Surveyed concave corner rib and range readings at 6-ft setup.

Shotcrete wall

Frame

Rib

KEY

———   ———   Approach line

0   1   2   ﹨3   4   5
Scale, ft
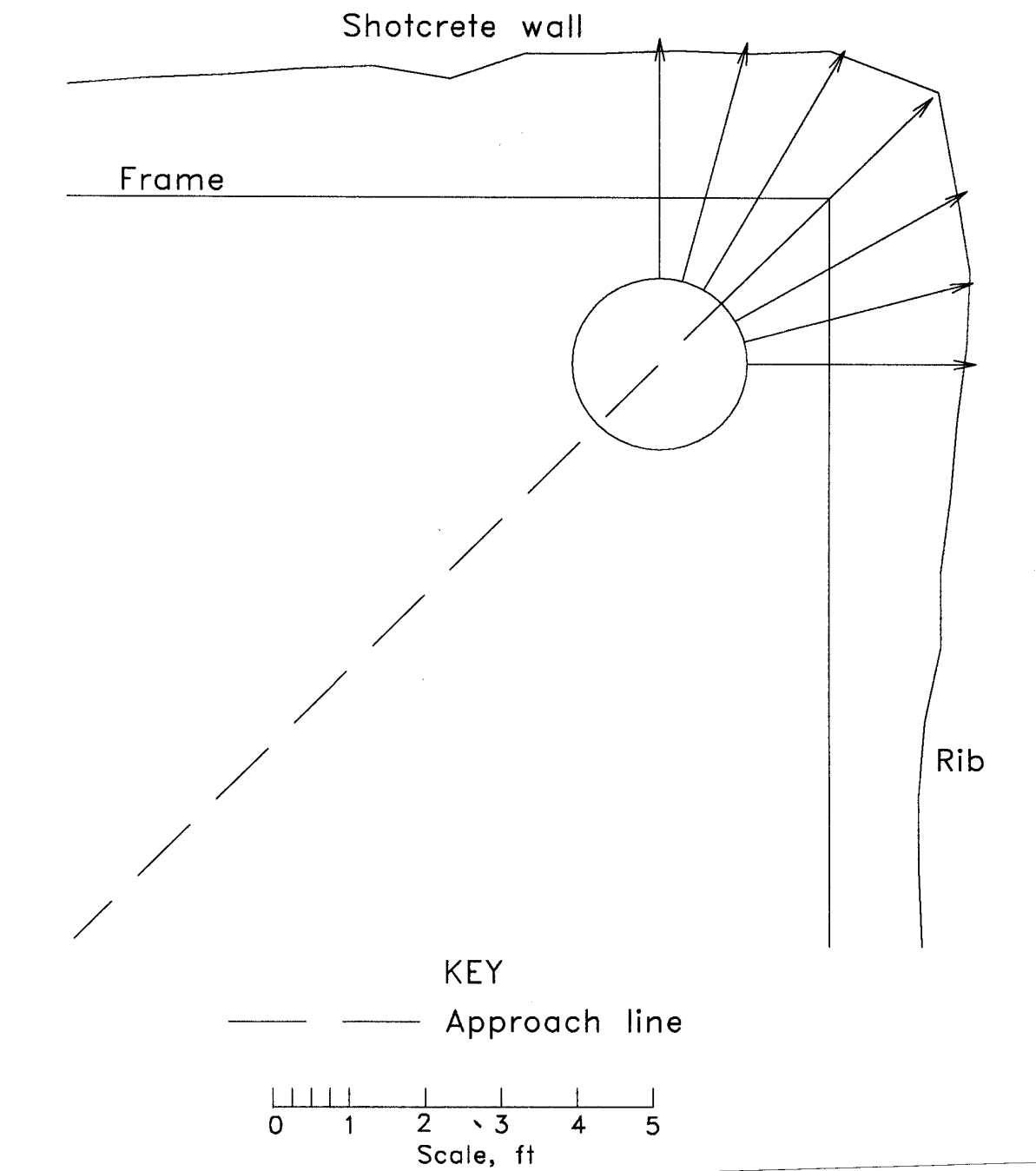
Figure 19.—Surveyed concave corner rib and range readings at 2-ft setup.
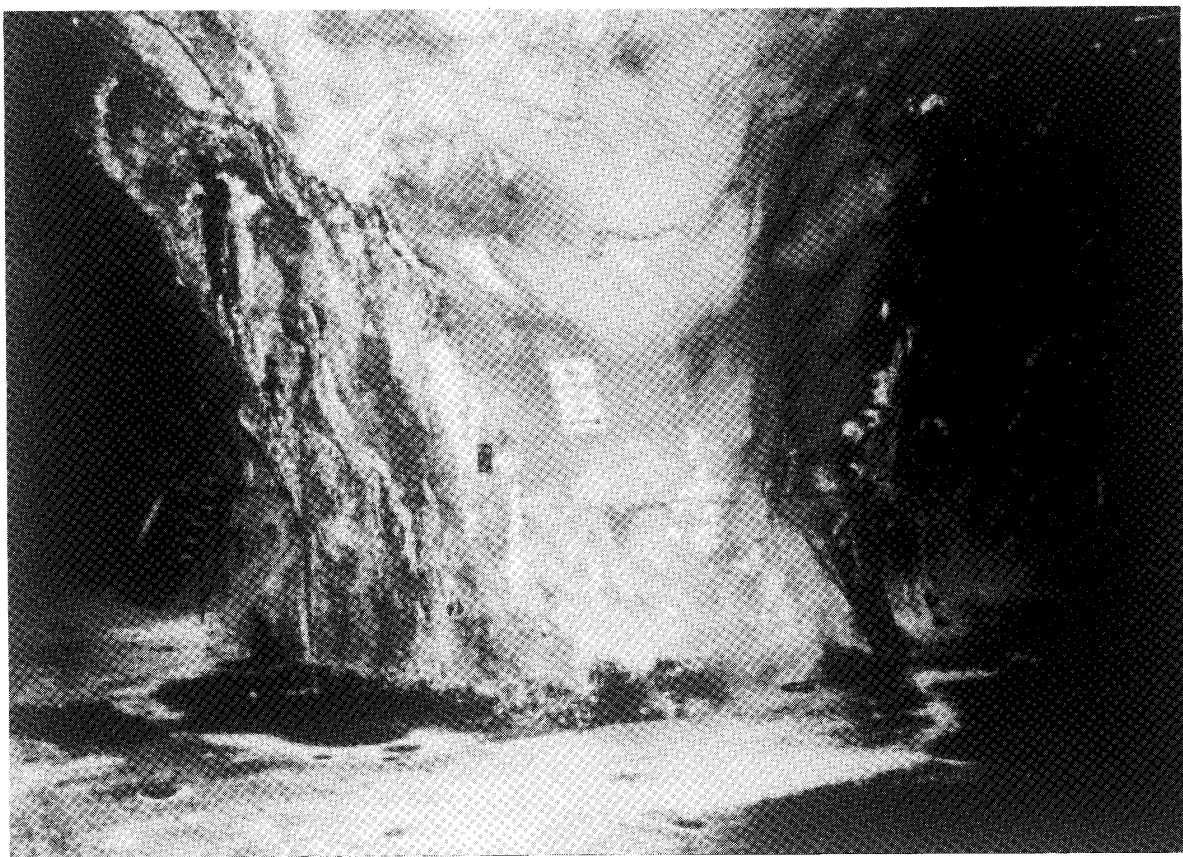
Figure 20.—Convex corner at Henderson Mine.

45°   90°   135°

0° —————————————————————————————

Rib

|⊔⊔⊔⊔_|___|___|___|___|
0   1   2   3   4   5
Scale, ft
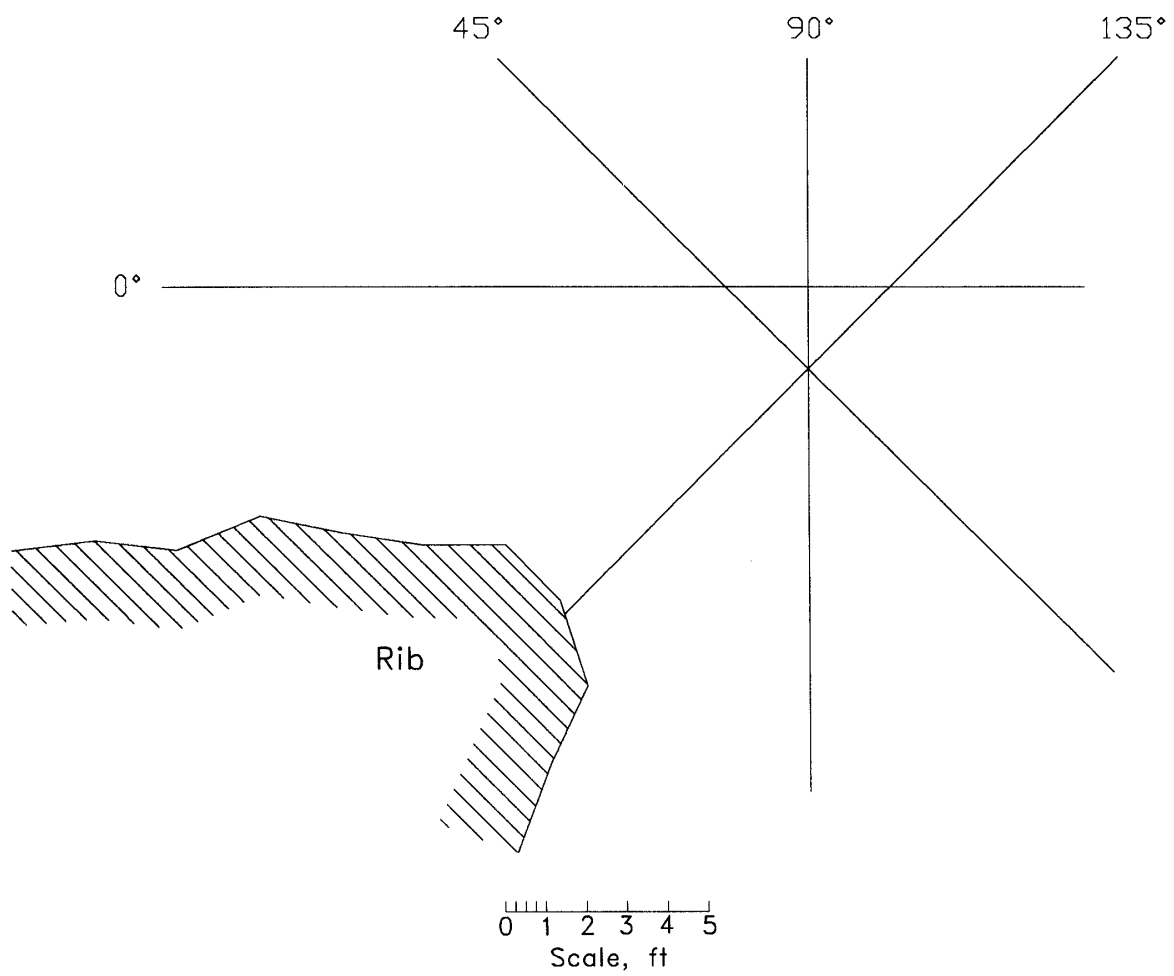
Figure 21.—Approach lines to convex corner.

Figure 22.—Sensor 6, 0° approach to convex corner.

Rib

KEY
● Rib survey point

0 1 2 3 4
Scale, ft

Direction of travel
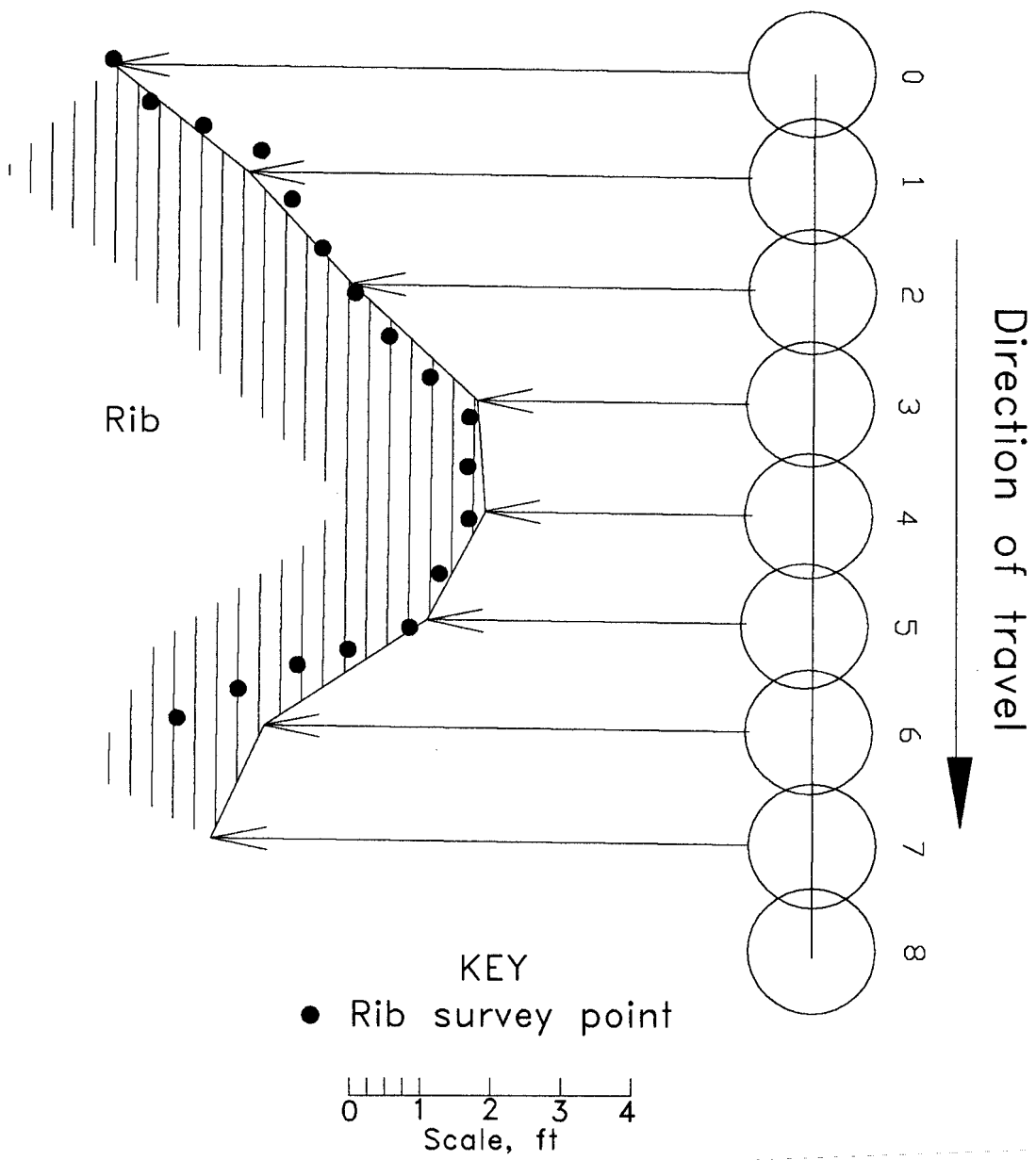
Figure 23.—Sensor 6, 45° approach to convex corner.

Direction of travel

0
1
2
3
4
5
6
7
8

Rib

KEY

● Rib survey point

0 1 2 3 4
Scale, ft

Figure 24.—Sensor 6, 90° approach to convex corner.
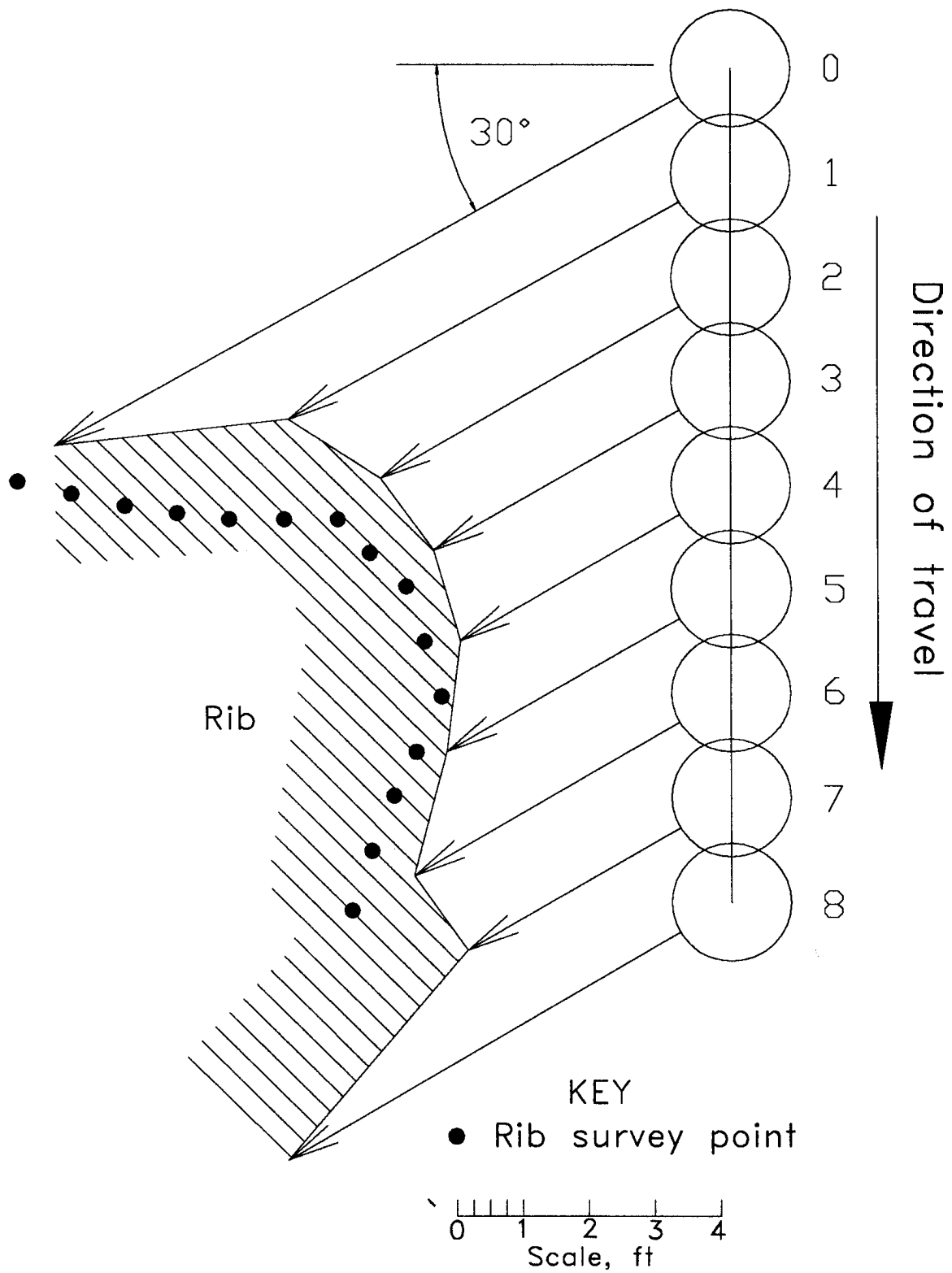
Figure 25.—Sensor 1, 90° approach to convex corner.

KEY

● Rib survey point
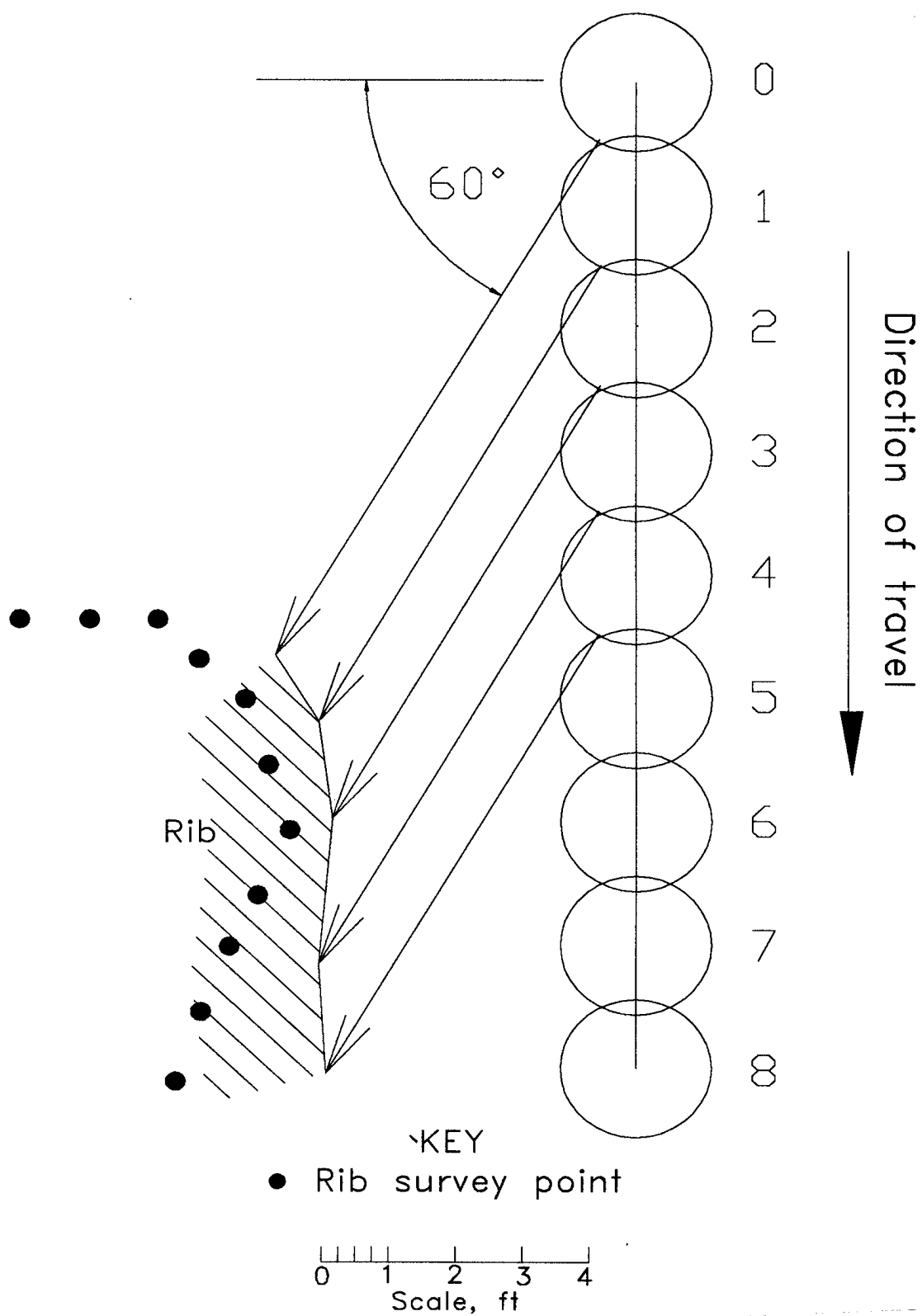
Figure 26.—Sensor 2, 90° approach to convex corner.
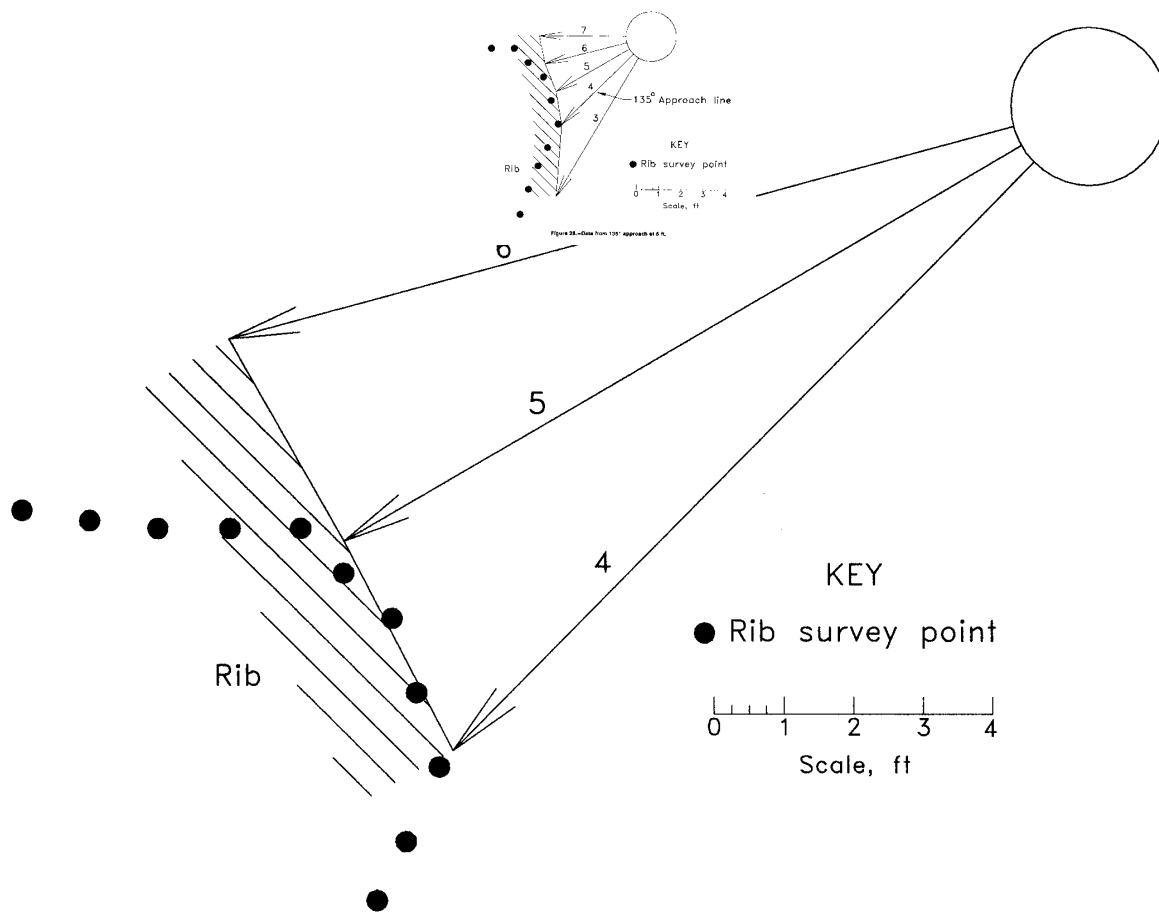
Figure 27.—Data from 135° approach at 14 ft.

Figure 28.—Data from 135° approach at 6 ft.

KEY

● Rib survey point

Scale, ft

Figures 29 through 32 show the intersecting ribs mapped by traditional surveying techniques as dotted lines, and the sonar rays of less than 25.5 ft as arrows. Range readings that were greater than or equal to 25.5 ft (the maximum for these rangers) were not plotted. The range data defined the convex corners at the intersection very well.

The next step in the intersection experiment was to push the Denning ring through the intersection at a nearly constant velocity without stop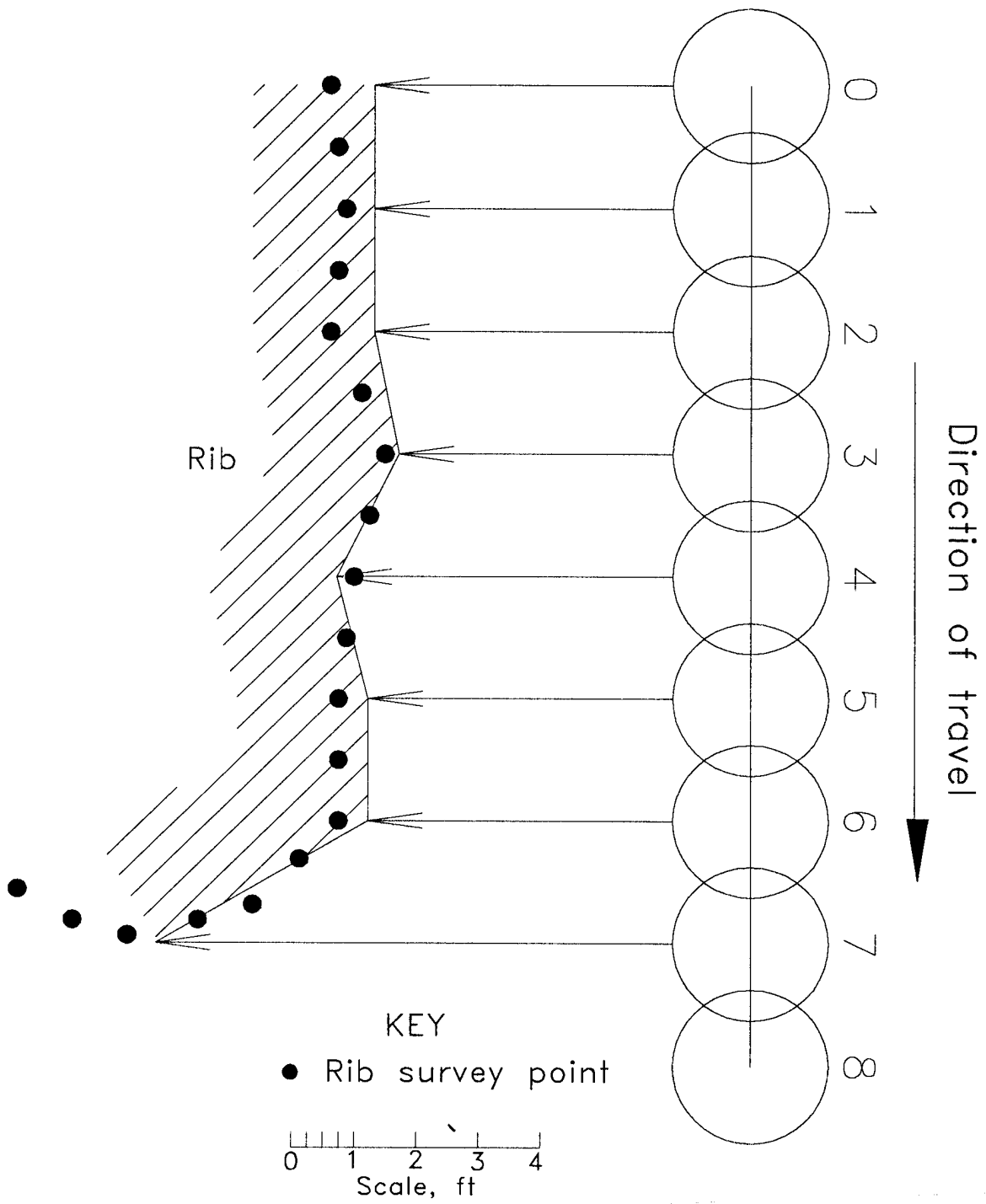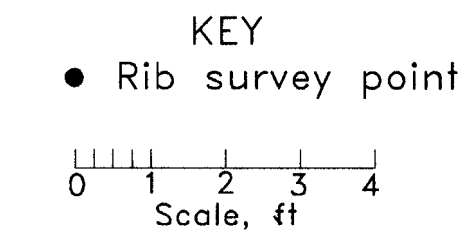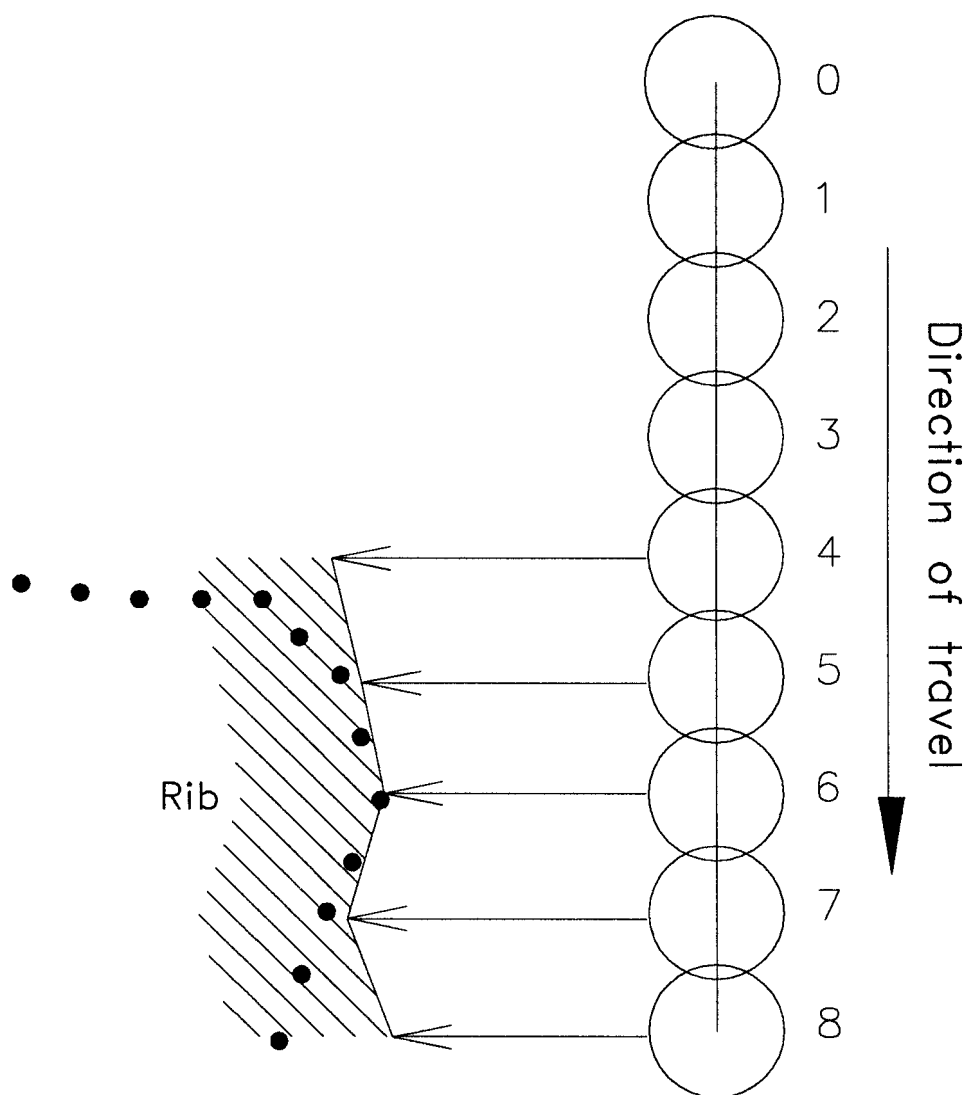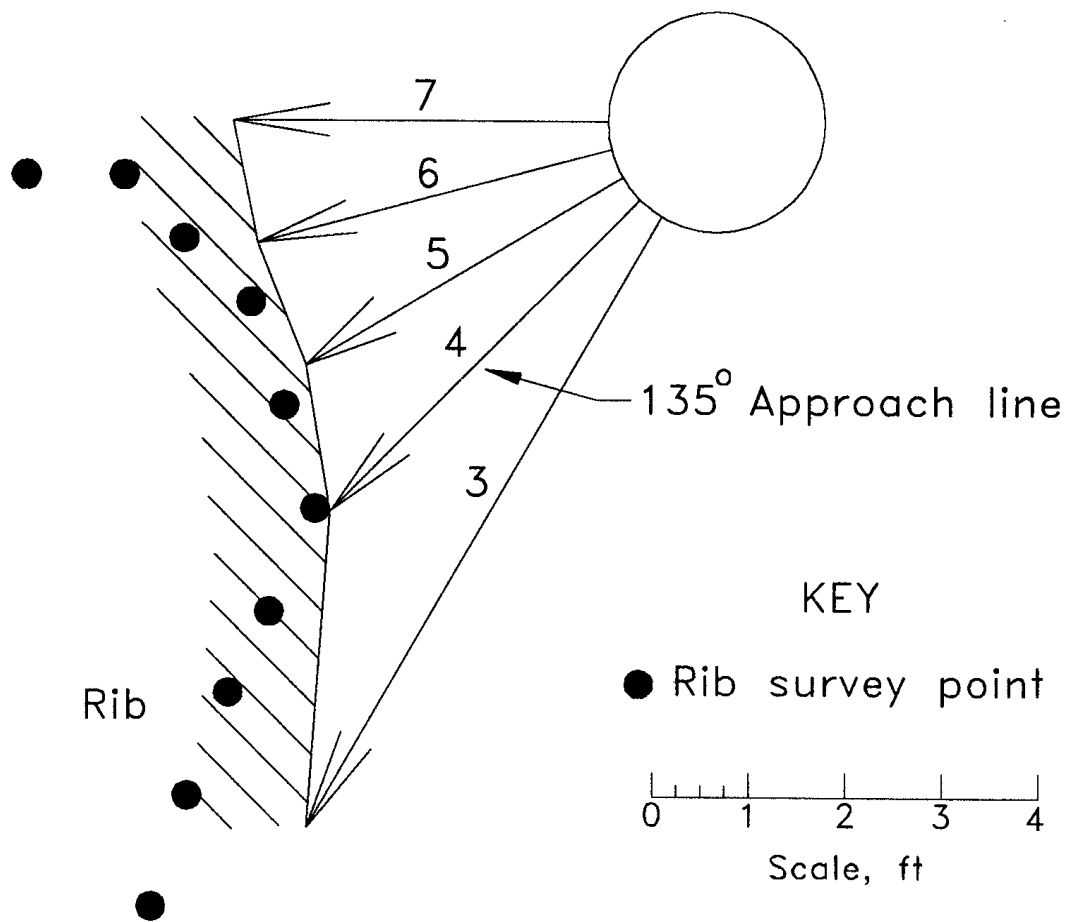ping every 2 ft to store data. Sensor 7 was aligned along the track centerline, and sensor 1 was aligned perpendicular to the rib line. The sensors pulsed constantly while the cart moved. Every complete cycle of ranger pulses can be used to produce a map of occupied and unoccupied regions. In this case, all the readings from sensor 1 were combined to build a map of the rib. Figure 33 shows the map compared to the actual survey.

A program has been written in Pascal, Ultraran.pas (see appendix), to automate the map building process. The program takes the data file from the Denning ring and produces an output file of data points for display in a common computer-aided drafting software package.

Table 2 shows a sample data output from the Denning ring. Ultraran.pas reads the Denning ring output file, places the range reading from each of the 24 sensors in an array, and eliminates the sensor identification characters.

Table 2.—Typical Denning ring output, 0.1 ft

Sensor	A	B	C	D	E	F	G	H
0 to 7	66	65	66	70	76	114	255	237
8 to 15	255	255	255	255	255	255	255	255
16 to 23 . . .	255	255	255	255	255	255	255	255

NOTE.—A = sensors 0, 8, 16; B = sensors 1, 9, 17; C = sensors 2, 10, 18; D = sensors 3, 11, 19; E = sensors 4, 12, 20; F = sensors 5, 13, 21; G = sensors 6, 14, 22; H = sensors 7, 15, 23.

Ultraran.pas uses the range array to compute coordinates of points that produced an echo detected by the Denning ring. The first step calculates the world coordinates of the ring each time it receives an echo. Then, the code computes rib point coordinates from the recorded ranges. The ring changed position for each row of data in the range array. The equations for updating the ring equations are

$$RingX[row] = \delta P \cdot \cos(RingAzimuth)$$
$$+ RingX[row -1],$$

and $\quad RingY[row] = \delta P \cdot \sin(RingAzimuth)$
$$+ RingY[row -1],$$

where: $RingX[row]$ = current X coordinate (ft) of the Denning ring,

$RingY[row]$ = current Y coordinate (ft) of the Denning ring,

$RingAzimuth$ = vehicle (cart) heading (degrees from true North),

$RingX[row -1]$ = previous Denning ring X coordinate (ft),

$RingY[row -1]$ = previous Denning ring Y coordinate (ft),

and $\qquad \delta P$ = distance traveled (ft) from the last reading.

$$\delta P = Vel \cdot \delta T$$

where $\quad \delta T$ = Denning ring interfire delay (s).

and $\quad Vel$ = vehicle (cart) velocity.

Ultraran.pas computes the rib point X and Y coordinates from the ring positions with the following equations:

$$X: = [Range/10 \cdot \cos(SensorRayAngle)] + RingX,$$

and $Y: = [Range/10 \cdot \sin(SensorRayAngle)] + RingY,$

where $\qquad X$ = rib point X coordinate (ft),

Y = rib point Y coordinate (ft),

$Range$ = range reading (ft) from the range array,

and $SensorRayAngle$ = azimuth (deg) of the sensor axis.

$$SensorRayAngle = [15 \cdot (KeyRanger - Transducer)$$
$$\cdot \pi/180] + RingAzimuth,$$

where $KeyRanger$ = number of the transducer pointing along the drift centerline,

and $Transducer$ = number of the transducer producing the range reading.

Figure 29.—Intersection as seen by sensor 1. Note: 9X and 94LD denote specific locations in the mine where this series of tests were conducted.

Figure 30.—Intersection as seen by sensor 2. Note: 9X and 94LD denote specific locations in the mine where this series of tests were conducted.

9X
¢

◄—— Direction of travel

−20 ft   +20 ft   94 LD
                                                    ¢
                                              60°

KEY

• Rib survey point

├┴┤─┴─┴─┴─┤
0 2 4 6 8 10
   Scale, ft

Figure 31.—Intersection as seen by sensor 3. Note: 9X and 94LD denote specific locations in the mine where this series of tests were conducted.

9X
¢

◄—— Direction of travel

−20 ft   −10 ft   +10 ft   +20 ft   94 LD
                                                        ¢
                                                  45°

KEY

• Rib survey point

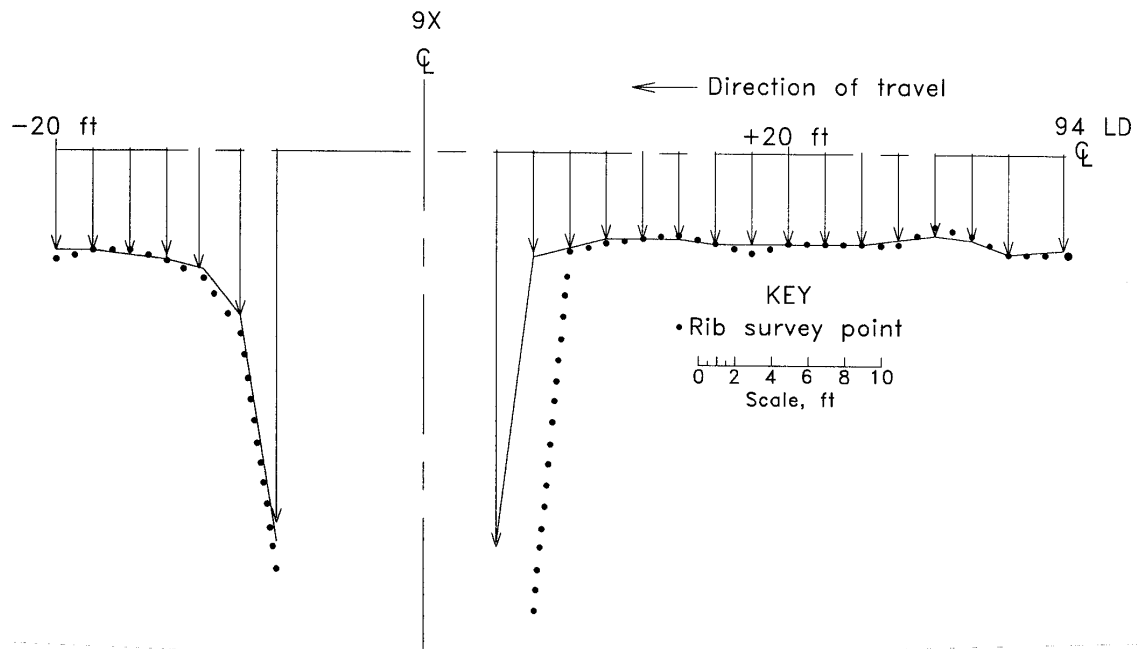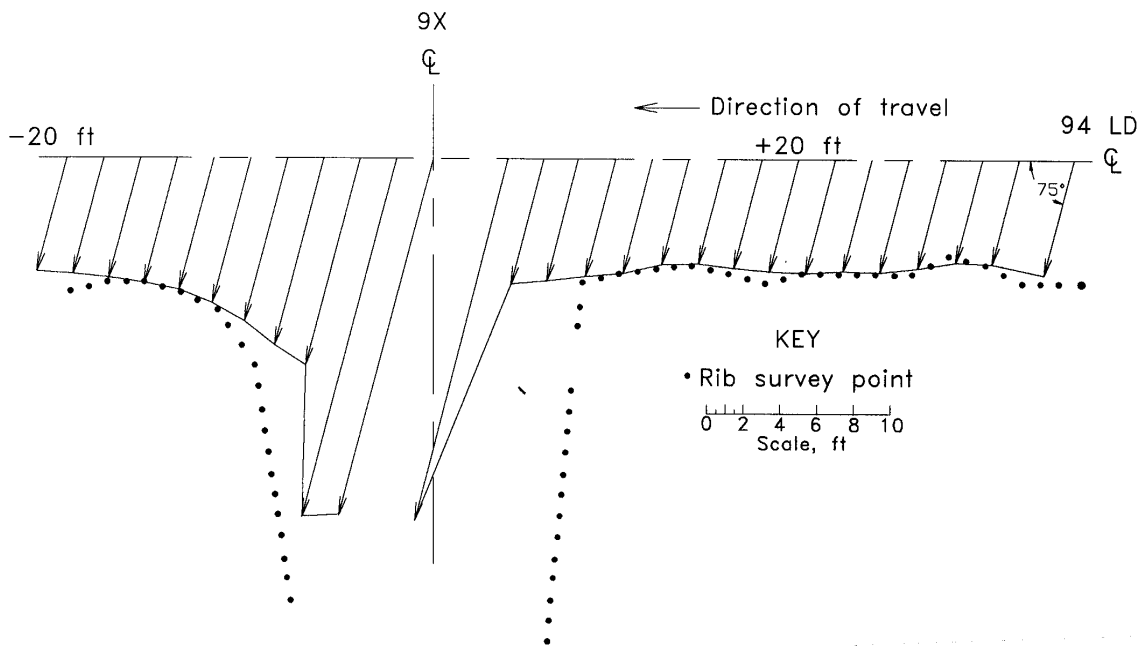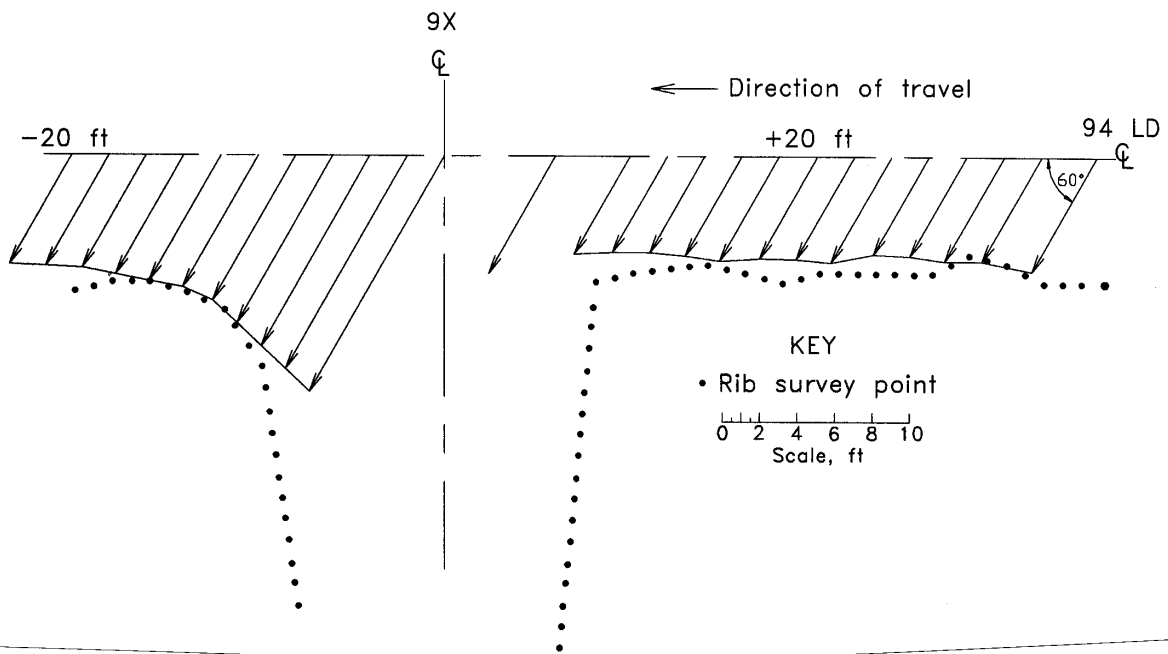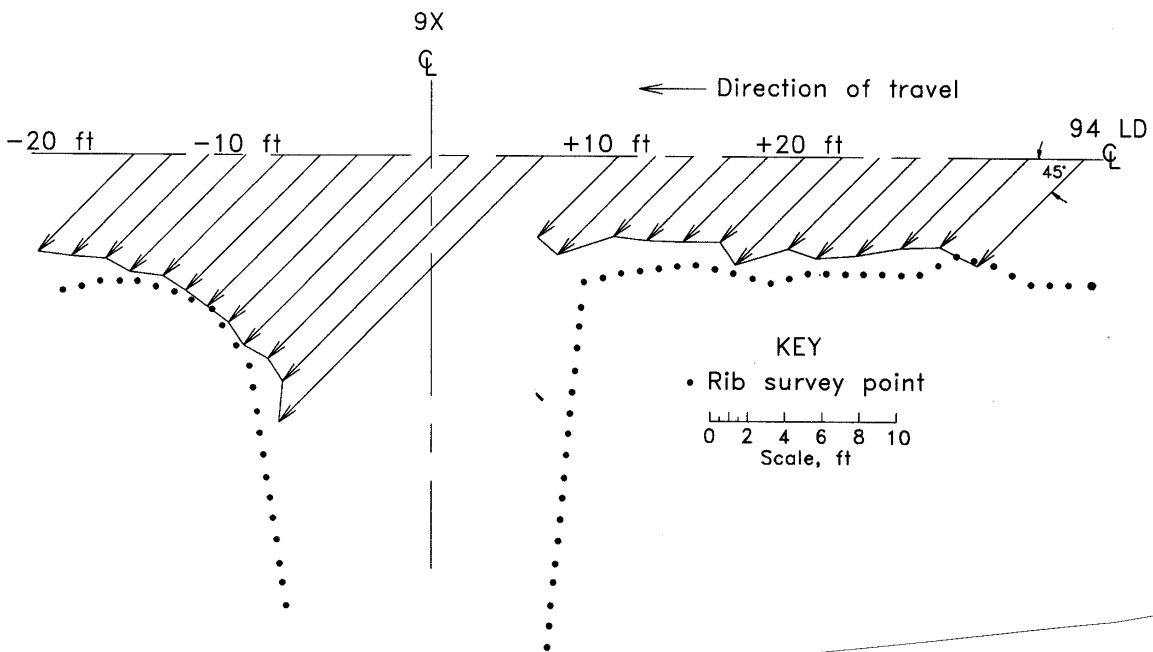├┴┤─┴─┴─┴─┤
0 2 4 6 8 10
   Scale, ft

Figure 32.—Intersection as seen by sensor 4. Note: 9X and 94LD denote specific locations in the mine where this series of tests were conducted.
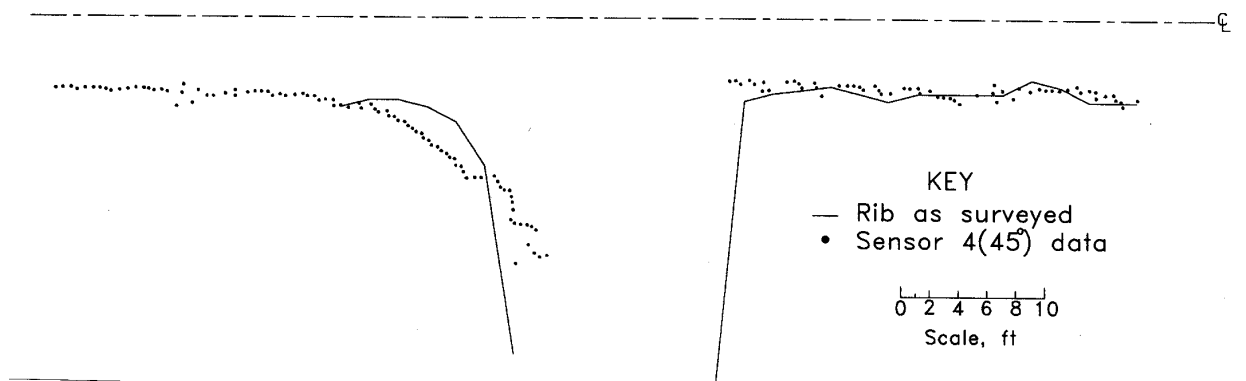
Figure 33.—Fly by view of intersection, sensor 4.

The occupied points (in this case, rib points) are written to a file with a *.dxf extension that can be read by the computer-aided drafting package for display and comparison. Figure 33 shows good correlation between the range readings and the surveyed rib line.

SENSOR DURABILITY

The ability of ultrasonic rangers to survive the mine environment is extremely important if they are to be used to navigate underground vehicles. The researchers mounted three Polaroid rangers and the circuitry for one ranger in a steel box (fig. 34) and bolted it to a production LHD. The LHD operated normally, exposing the sensor faces to the environment, and all components in the box to shock and vibration.

The rangers were removed and tested after 68 h of production exposure. Two of the rangers gave reliable range readings, even though they were covered with dust. The gold foil on the third was ripped, probably by a sharp object such as a rock, causing sensor failure. The remaining two rangers on the LHD were replaced, along with a replacement for the failed ranger, for another 149 h of operation. Again, one of these rangers failed after being struck in the faceplate. The impact broke the plastic frame of the ranger, and forced the faceplate into the foil. The other rangers continued to give accurate range readings.

The final durability test lasted 287 additional operating hours. This time, all three rangers survived in good condition and produced accurate range readings when tested. There were no failures in the analog or digital ranging circuit boards stored in the enclosure during the tests.

Several different enclosures were tested to protect the frame and faceplate of the Polaroid rangers in the laboratory. The first unit tested was Polaroid's Environmental Enclosure, marketed for use in industrial environments. The grill is made of Valox resin (fig. 35) and is specially tuned to reduce interference with the sonar beam. However, this plastic covering cannot withstand direct impacts by rocks.

Protective enclosures were fabricated from plastic-coated 1/2-in wire mesh and 1/4-in expanded metal (fig. 35), and were mounted 1/8 in from the face of the sensor, within blanking zone.

The results of range and FOV tests (table 3) show that none of the grills placed at this position severely degraded ranger operation. However, the grills are seen as an object in the FOV when they are placed more than 3/4 in from the ranger face. Protective covers such as these should improve the Polaroid ranger's resistance to impact. It may also be possible to mount the ranger in such a way that the sound wave is reflected in the desired direction by bouncing it off a metal or plastic plate, while the ranger itself remains protected within the housing. This arrangement was not tried, but it would probably reduce echo strength.

Table 3.—Range and field-of-view tests with protective grills

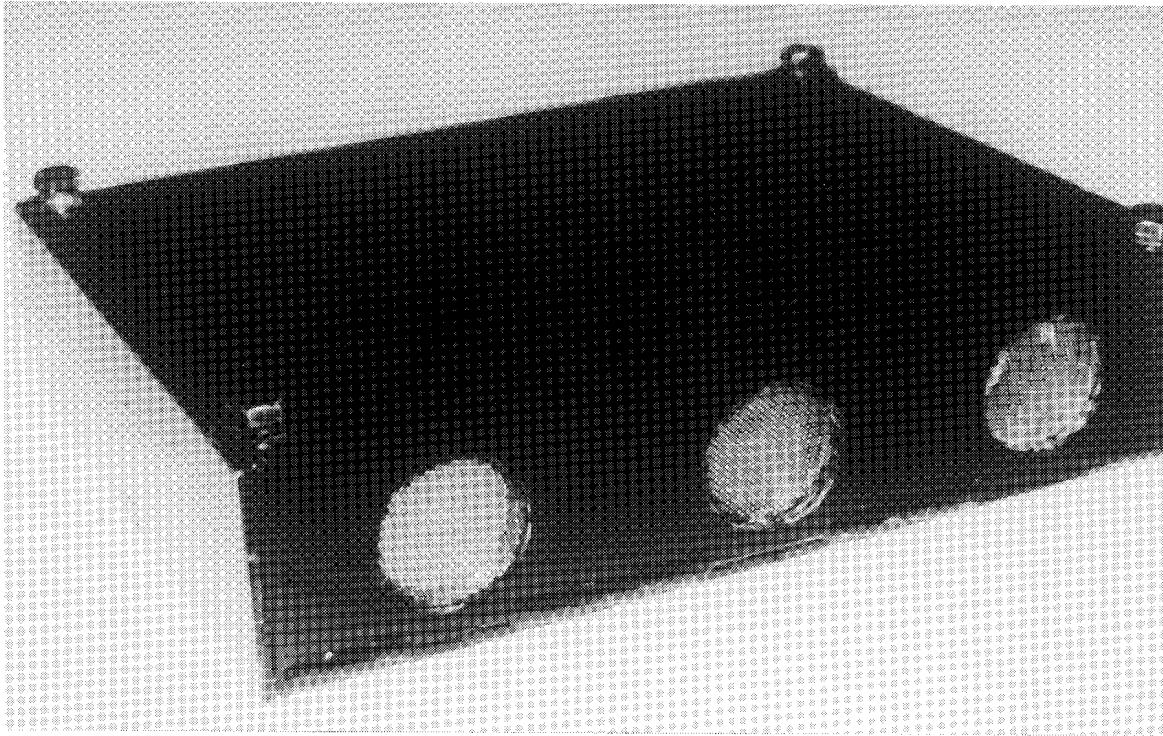| Measured distance to dowel, ft	Polaroid test enclosure		1/4-in expanded metal		1/2-in wire mesh	
	Range, ft	FOV, deg	Range, ft	FOV, deg	Range, ft	FOV, deg
2.5	2.5	0	2.5	0	2.5	0
5.0	5.0	19.9	5.0	23.1	5.0	22.1
7.5	7.5	0	7.5	0	7.5	0
10.0	9.9	16.5	9.9	17.7	10.0	18.2
12.5	12.4	0	12.4	0	12.5	0
15.0	14.9	14.6	14.8	15.0	14.9	16.6

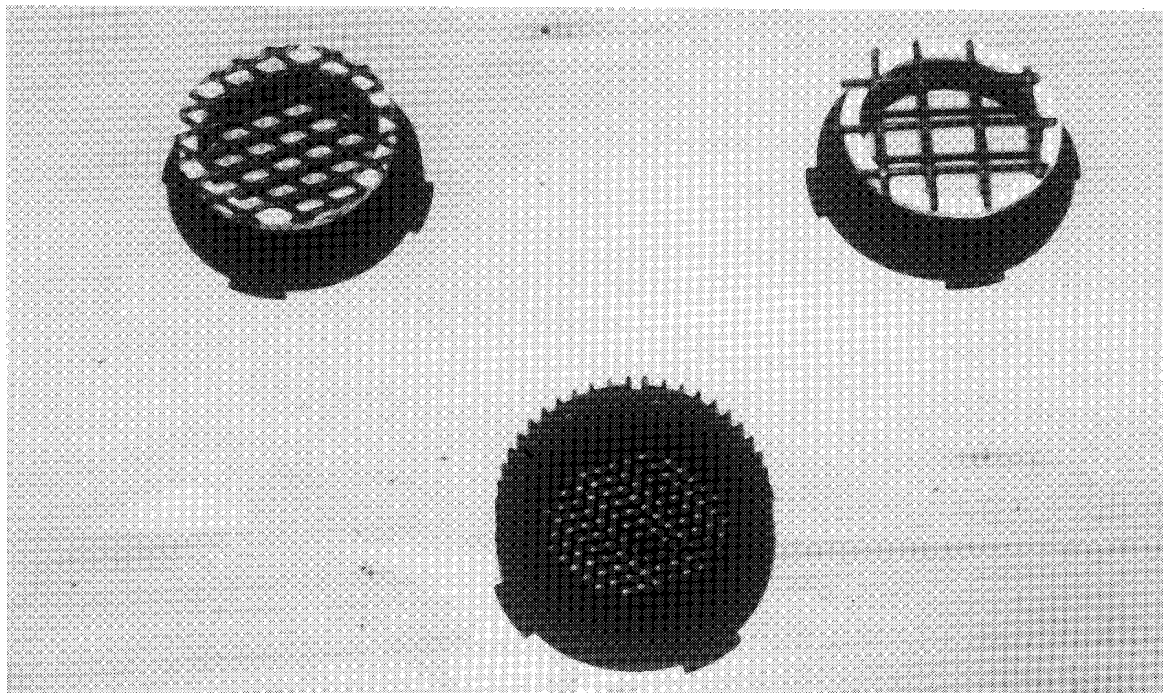Figure 34.—Enclosure for mounting sensors on production load-haul-dump.

Figure 35.—Protective faceplates for sensors (upper left = 1/4-in expanded metal, upper right = 1/2-in wire mesh, middle = Polaroid design).

Some ultrasonic rangers, such as the Milltronics ST-25 and ST-100 rangers, are designed for severe environments (26). Milltronics coats these piezoelectric transducers with polyurethane to protect them from dust, water, and abrasion. They are designed to withstand shock, and because they are piezoelectric, there is no polyester film foil to rip. They have been field proven in applications with dust, steam, and acids, and have been used to reliably detect live ore storage levels under the main gyratory crusher at the Henderson Mine. The Milltronics ST-25 ranger has a rated beam width of 12°, and the ST-100 ranger has a beam width of 7° (28). They appear to be more rugged and have better beam angles; they will be tested in the future.

CONCLUSIONS

This study showed that ultrasonic rangers can identify mine rib navigation features and can provide adequate data for computer-aided mining vehicle guidance. The rangers defined convex corners, concave corners, intersections, and roughly linear planes when the incidence angle was appropriate. Ultrasonic rangers will probably not give all the data needed for navigation of a computer-aided vehicle. For instance, in their present form, ultrasonic rangers cannot fully define all the features of a muck pile. However, they give simple range data that can identify common mine features with a good deal of clarity. To give all the information a vehicle needs for navigation, a suite of sensors will be required.

Large angles of incidence (greater than 60°), combined with the FOV, caused improper definition of the rib line. The rangers did not completely define the rib intersection point of concave corners in all cases. The rangers did, however, measure the distance to this wide range of objects with adequate precision to define the mine's features for a computer-guided vehicle.

Underground mine features appear to be excellent sound reflectors. Because they are rough, they diffuse the sound energy so multiple strong reflections and deflections are not present, and because they are hard and solid, they absorb very little sound energy. Because mine ribs are so rough, they provide enough surface area that is nearly perpendicular to the sensor axis for the rangers to work well with relatively large angles of incidence. The only time the rock roughness created problems was when the transmit burst hit at an extremely high angle of incidence. When this event occurred, high data variability resulted, because the roughness intermittently reflected enough energy from the transmit wave's edges to trigger the ranger amplitude threshold. This problem may be approached by recognizing patterns in the echo waveform.

The rangers were sensitive to small objects protruding from the ribs, since 1/2-in rock bolts reflected enough energy to trigger the amplitude threshold. Consequently, the bolts formed part of the rib outline map produced from ranger data. This might be considered an error in object recognition, but the rib outline that resulted would help prevent collision between computer-guided vehicles and the rib, protruding bolts, or any other obstacle.

The rangers that were mounted on a production LHD withstood everything in the mine environment except direct hits from sharp objects like rocks. The rangers are durable enough for mine operating conditions that include extremes in vibration, dust, and humidity. Experiments showed that faceplate protection can be added to the mounting without creating serious sound wave attenuation problems.

Certain types of piezoelectric ultrasonic rangers, such as the Milltronics unit described, can probably survive the mine environment even better than the electrostatic sensors tested in these experiments.

A thorough knowledge of the task the ultrasonic range sensor is to perform and the ranger's individual characteristics is important. When used incorrectly, the rangers do not provide reliable data.

REFERENCES

1. Oppenheim, I. J., and W. L. Whittaker. Demonstration of Robotic Mapping of Mine Spaces. Civ. Eng. Robotics Lab. Rep. Carnegie Mellon Univ., Pittsburgh, PA, 1985, 11 pp.

2. Urick, R. J. Principles of Underwater Sound. McGraw-Hill, New York, NY, 1975, 384 pp.

3. Sutton, J. L. Underwater Acoustic Imaging. Modern Acoustical Imaging, ed. by H. Lee and G. Wade. IEEE, New York, NY, 1986, pp. 229-241.

4. Crowley, J. L. Dynamic World Modeling for an Intelligent Mobile Robot Using a Rotating Ultra-Sonic Ranging Device. Carnegie Mellon Univ. Robotics Inst. Rep. CMU-RI-TR-84-27, Pittsburgh, PA, 1984, 17 pp.

5. Drumheller, M. Mobile Robot Localization Using Sonar. IEEE Trans. Pattern Anal. and Mach. Intell., v. 9, No. 2, March 1987, pp. 325-332.

6. Elfes, A. A Sonar-Based Mapping and Navigation System. Paper in IEEE Robotics and Automation Conference Proceedings. IEEE CH2282-2/86/0000/1151, 1986, pp. 1151-1156.

7. ____. Sonar-Based Real-World Mapping and Navigation. IEEE J. Robotics and Autom., v. 3, No. 3, June 1987, pp. 249-265.

8. Moravec, H. P., and A. Elfes. High Resolution Maps From Wide Angle Sonar. Paper in IEEE Robotics and Automation Conference Proceedings. IEEE CH2152-7/85/0000/0116, 1985, pp. 116-121.

9. Walter, S. The Sonar Ring: Obstacle Detection for a Mobile Robot. Paper in IEEE Robotics and Automation Conference Proceedings. IEEE CH2413-3/87/0000/1574, March 1987, pp. 1574-1579.

10. Denning Mobile Robotics (Wilmington, MA). Denning Ring Operating Manual. 1987, 98 pp.

11. Doepken, W. G. The Henderson Mine. Ch. in Underground Mining Methods Handbook. W. A. Hustrulid, New York, NY, AIME, 1982, pp. 990-997.

12. Everett, H. R. Survey of Collision Avoidance and Ranging Sensors for Mobile Robots. Nav. Ocean Syst. Cent., Tech. Rep. No. 1194, San Diego, CA, 1987, 179 pp.

13. Campbell, D. Ultrasonic Noncontact Dimensional Measurement. Sensors, v. 3, July 1986, pp. 37-43.

14. Biber, C., S. Ellin, E. Shenk, and J. Stempeck. The Polaroid Ultrasonic Ranging System. Paper in Preprint of the Sixty-seventh Convention of the Audio Engineering Society. Audio Eng. Soc., New York, NY, 1980, 11 pp.

15. Pierce, A. D. Acoustics—An Introduction to its Physical Principles and Applications. McGraw-Hill, New York, NY, 1981, 642 pp.

16. Chande, P. K., and P. C. Sharma. A Fully Compensated Digital Ultrasonic Sensor for Distance Measurement. IEEE Trans. Instrum. and Meas., v. 3, No. 2, 1984, pp. 128-129.

17. Meyer, E., and E. G. Neumann. Physical and Applied Acoustics—An Introduction. Academic, New York, NY, 1972, 412 pp.

18. Kinsler, L. E., A. R. Frey, A. B. Coppens, and J. V. Sanders. Fundamentals of Acoustics. Wiley, New York, NY, 1982, 524 pp.

19. Brown, M. K. Feature Extraction Techniques for Recognizing Solid Objects with an Ultrasonic Range Sensor. IEEE J. Robotics and Autom., v. 1, No. 5, 1985, pp. 191-205.

20. Bass, H. E., L. C. Sutherland, J. Piercy, and L. Evans. Absorption of Sound by the Atmosphere. Physical Acoustics, ed. by W. P. Mason and R. N. Thurston. Academic, v. XVII, New York, NY, 1984, 326 pp.

21. Polaroid Corporation (Cambridge, MA). Ultrasonic Ranging System. Ultrasonic Ranging Marketing Div., 1982, 34 pp.

22. Cooper, W. E., D. D. Rapp, and J. B. Hudgins. Noise Investigation—Cannon Mine. MSHA Rep. D-5903 P-588, Denver, CO, 1987, 20 pp.

23. Kuc, R., and M. W. Siegel. Efficient Representation of Reflecting Structures for a Sonar Navigation Model. Paper in IEEE Robotics and Automation Conference Proceedings. IEEE CH2413-3/87/0000/1916, March 1987, pp. 1916-1923.

24. Borenstein, J., and Y. Koren. Obstacle Avoidance with Ultrasonic Sensors. IEEE J. Robotics and Autom., v. 4, No. 2, April 1988, pp. 213-218.

25. King, R., and A. Gordon. Intelligent Waveform Analysis for Ultrasonic Ranging in a Cluttered Environment. CO Inst. Artificial Intell., Univ. CO at Boulder, April 1990, 18 pp.

26. Milltronics (Arlington, TX). MultiRanger Plus Product Catalogue. 1989, 6 pp.

APPENDIX.—PROGRAM FOR CONVERTING DATA FROM DENNING RING

The following program, Ultraran.pas, is written in Turbo Pascal. The program accepts the output file from the Denning ring, and converts it to points in a .dxf file that can be interpreted by computer-aided software packages.

```
{$R+}
Program UltraRange (input, output, InputFile, OutputFile);
```

{This program accepts data from a file generated by a moving Denning ring and computes X,Y positions of the objects that reflect the ultrasonic waves.}

```
var
        StartX, StartY: real;            {Denning ring starting coordinates}
        Vel: real;                       {Denning ring velocity}
        DeltaT: real;                    {Time interval between range readings}
        Dist:real;                       {Distance that the Denning ring moved during the test}
Procedure EnterTestParameters (var StartX, StartY, Vel, DeltaT: real);
```

{This procedure enters the information that describes the Denning ring setup and calculates the total number of readings.}

```
Begin
        writeln ('Enter the starting X coordinate of the Denning ring [0].');
        readln (StartX);
        writeln ('Enter the starting Y coordinate of the Denning ring [0].');
        readln (StartY);
        writeln ('Enter the velocity of the Denning ring in ft/sec [0.8].');
        readln (Vel);
        writeln ('Enter the time interval in sec. between range readings [0.075].');
        readln (DeltaT);
        End; {EnterTestParameters}

Procedure ReadAndWriteThreeLines(reading:integer;
                 InputFileName, OutputFileName:string;
                                     var ch:char;
                 var InputFile, OutputFile:text);
```

{This procedure reads the characters and range values in the 3 lines of the input file that contain data from all 24 sensors. It writes the range readings to a file of 1 reading of 24 sensors per row.}

```
        type RangeArray=array [1..200, 1..25] of integer;

        var Range: RangeArray;           {Range readings extracted from the Denning file and read to OutputFile}
        sensor:integer;                  {Each column in the new range array is for a sensor; each row is a reading}
        LineNumber:integer;              {Represents the three lines of sensor data per reading}
        First, Last:integer;             {The numbers of the first and last sensors in the three lines}

Begin
        First:=1;                        {The first sensor number in the line}
        Last:=8;                         {The last sensor number in the line}
```

```
          LineNumber:=1;
          while (LineNumber<=3) and not (eof(InputFile) or (ch='>'))
                    do begin
                    repeat
                    read (InputFile, ch);
                    write (ch);
                    until (ch=']') or (ch='>') or eof(InputFile);
```

{"]" is the last character in the string that is to be omitted from the range array.}

```
                    LineNumber:=LineNumber+1;
                    Sensor:=First;
                    while (Sensor <= Last) and not eof(InputFile) and not (ch='>')
                    do begin                   {Read range values into OutputFile}
                    read (InputFile, Range [reading, sensor]);
                    write (OutputFile, Range [reading, sensor]:4);
                    writeln(Range[reading,sensor],',',
                    reading,',',sensor);
                    sensor:=sensor+1;
                    end;{while sensor <= Last}
                    First:=First+8;
                    Last:=Last+8
                    end; {while LineNumber <= 3}
End; {ReadAndWriteThreeLines}
```

Procedure ExtractRangeData;

{The Denning ring writes range data via an RS232 link to a PC file. This procedure removes initial characters from the file, for example, [0-7], that identify the sensors, and writes the integer range values to the output file for further processing.}

```
          var ch:char;                {Character variable for reading the sensor identifiers that are being removed
                                          from the range data}
          InputFile:text;             {The Denning ring file of raw data}
          OutputFile:text;            {The file of range values produced by this procedure}
          InputFileName:string[45];
          OutputFileName:string[45];
          reading:integer;            {Each line in the new range array is a reading}

          Begin
                    writeln ('Please enter the name of the file produced by the');
                    write ('Denning Ring that will be input to this program.>>');
                    readln (InputFileName);
                    assign (InputFile, InputFileName);
                    reset (InputFile);
                    write ('What do you want to name the output file?>>');
                    readln (OutputFileName);
                    assign (OutputFile, OutputFileName);
                    rewrite (OutputFile);
                    reading:=1;
                    ch:=' ';
          while (not eof (InputFile)) and (not (ch='>')) do begin
                    ReadAndWriteThreeLines(reading, InputFileName, OutputFileName,
                      ch, InputFile, OutputFile);
```

```
                    writeln (OutputFile);
                    reading:=reading+1
                  end; {while not eof}
                    close (InputFile);
                    close (OutputFile);
                  end; {ExtractRangeData}
Begin

         StartX:=0.0; StartY:=0.0; Vel:=0.8; DeltaT:=0.075;
         EnterTestParameters (StartX, StartY, Vel, DeltaT);
         ExtractRangeData;
End.
```